Department of Probability and Mathematical Statistics
Faculty of Mathematics and Physics
Charles University in Prague, Czech Republic

Univerzita Karlova v Praze

Matematicko-fyzikální fakulta

DIPLOMOVÁ PRÁCE

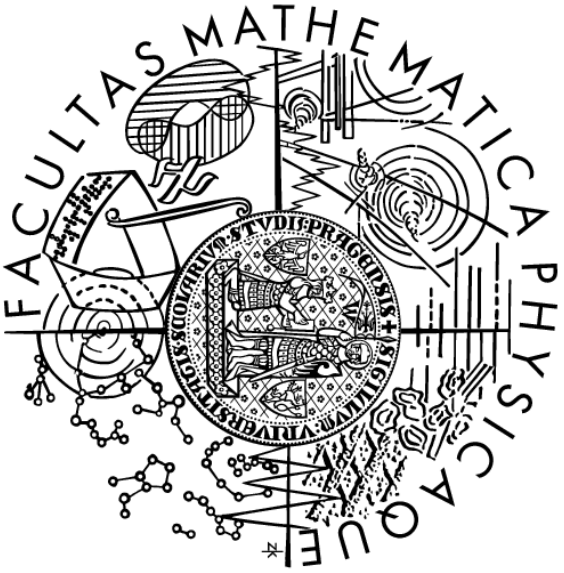

Verchiere Didier

Third order moment characteristics for spatial point processes
-
Momentové charakteristiky třetího řádu pro prostorové bodové procesy

MFF UK

Vedoucí diplomové práce: RNDr. Michaela Prokešová, Ph.D.

Studijní program: Matematika

Studijní obor: Pravděpodobnost, matematická statistika a ekonometrie

Katedra pravděpodobnosti a matematické statistiky

2010

Poděkování

Na tomto místě bych rád vyjádřil své poděkování všem, kteří mi při zpracování mé diplomové práce pomáhali. Především RNDr. Michaele Prokešové, Ph.D., za odborné vedení, názory a kritické i pochvalné připomínky. Dále také panu RNDr. Zbyňku Pawlasovi, Ph.D., za jeho trpělivost a čas, který mi věnoval. Děkuji za jeho cenné rady, které mi pomohly uvést práci do finální podoby. Nemohu opomenout ani Prof. RNDr. Viktora Beneše, DrSc., RNDr. Martina Mádlíka za jeho rady při programování a Mgr. Jiřího Dvořáka za zapůjčení programu na simulování LGCP.

Prohlašuji, že jsem svou diplomovou práci napsal samostatně a výhradně s použitím citovaných pramenů. Souhlasím se zapůjčováním práce.

V Praze dne

Contents

Název práce: Momentové charakteristiky třetího řádu pro prostorové bodové procesy
Autor: Verchière Didier
Katedra (ústav): Katedra pravděpodobnosti a matematické statistiky
Vedoucí diplomové práce: RNDr. Michaela Prokešová, Ph.D.
E-mail vedoucího: Michaela.Prokesova@mff.cuni.cz

Abstrakt: Při popisu a statistické analýze prostorových bodových procesů se velmi často používají momentové charakteristiky - tj. charakteristiky založené na momentech rozdělení počtu bodů bodového procesu pozorovaných v daných podmnožinách prostoru, na kterém je bodový proces definován. Nicméně standardně používané a tedy dobře prozkoumané jsou pouze charakteristiky prvního a druhého řádu jako například intenzita (popisující průměrný počet bodů v dané množině) či párová korelační funkce (popisující korelaci mezi přítomností dvou bodů procesu ve dvou pevně zvolených lokacích). Tyto charakteristiky jsou ovšem schopné postihnout jen část prostorových interakcí v bodovém procesu. Více interakcí mohou zahrnout charakteristiky třetího řádu.

V literatuře byly zatím navrženy a zkoumány dvě různé charakteristiky třetího řádu - takzvaná T-funkce (Schladitz, Baddeley 2000) a z-funkce (Moller et. al. 98).

Uchazeč se seznámí se základy teorie prostorových bodových procesů a s navrženými dvěma charakteristikami. Bude zkoumat jejich vlastnosti a možné metody odhadu těchto charakteristik. Rovněž bude diskutovat rozdíly mezi nimi a určí hodnoty těchto charakteristik pro různé druhy jednoduchých bodových procesů.

Klíčová slova: T-funkce, z-funkce, momentové charakteristiky třetího řádu.

Title: Third order moment characteristics for spatial point processes
Author: Verchière Didier
Department: Probability and Mathematical Statistics
Supervisor: RNDr. Michaela Prokešová, Ph.D.
Supervisor's e-mail address: Michaela.Prokesova@mff.cuni.cz

Abstract: Moment characteristics are widely used for the statistical analysis of spatial point processes. Standard summary statistics used for the analysis of point processes are of first and second order (intensity, K-function, pair-correlation function...). Nonetheless, none of these characteristics describes the distribution of a point pattern completely. Higher order characteristics such as third-order characteristics can give more information about the spatial interactions. Two such characteristics have already been studied: the z-function (Moller et. al. 98) and the T-function (Schladitz, Baddeley 2000).

Key words: T-function, z-function, third order moment characteristics.

Notations

$\emptyset$	the empty set;
$\mathbb{N}$	the positive integers;
$\mathbb{R}=(-\infty,\infty)$	the real line;
$\mathbb{R}^+=[0,+\infty)$	the positive real line;
$(a,b)=\{x\in\mathbb{R}: a<x<b\}$, for $a\in\mathbb{R}, b\in\mathbb{R}$	the opened interval;
$[a,b]=\{x\in\mathbb{R}: a\le x\le b\}$, for $a\in\mathbb{R}, b\in\mathbb{R}$	the closed interval;
$A\cup B=\{x\in S: x\in A\vee x\in B\}$, for $A\subset S$, $B\subset S$	the union;
$A\cap B=\{x\in S: x\in A\wedge x\in B\}$, for $A\subset S$, $B\subset S$	the intersection;
$A\setminus B=\{x\in S: x\in A\wedge x\notin B\}$, for $A\subset S$, $B\subset S$	the difference;
$A^c=\{x\in S: x\notin A\}$, for $A\subset S$	the complement;
$A_1\times\ldots\times A_n=\{(a_1,\ldots,a_n): a_1\in A_1,\ldots,a_n\in A_n\}$	the Cartesian product;
$\mathbb{R}^n$	the d-dimensional Euclidian space;
$\|x-y\|=\sqrt{(x_1-y_1)^2+\ldots+(x_n-y_n)^2}$	the Euclidian metric on $\mathbb{R}^n$;
$b(x,r)=\{y\in\mathbb{R}^n: \|x-y\|\le r\}$	the closed ball of radius r and centre x;
$\bar{b}(x,r)=\{y\in\mathbb{R}^n: \|x-y\|\le r\}\setminus\{x\}$	the closed ball without the centre;
$\partial b(x,r)=\{y\in\mathbb{R}^n: \|x-y\|=r\}$	the boundary of $b(x,r)$;
ω_d	the volume of the unit ball in $\mathbb{R}^d$;
$x+y=(x_1+y_1,\ldots,x_n+y_n)$, for $(x,y)\in(\mathbb{R}^n)^2$	the sum of vectors;
$c\cdot x=(c\cdot x_1,\ldots,c\cdot x_n)$, for $x\in\mathbb{R}^n$ and $c\in\mathbb{R}$	the multiplication of a vector by a constant;
$W_x=W+x=\{w+x: w\in W\}$, for $x\in\mathbb{R}^n$ and $W\subset\mathbb{R}^n$	the translated set;
$W_{-b(0,r)}=\{x\in W: inf\ \|x-y\|\ge r$ for any $y\in\partial W\}$	the eroded set;
$1_{[x\in A]}=\begin{cases}1 & \text{for } x\in A\\ 0 & \text{otherwise}\end{cases}$	the indicator function of a measurable set A;
ℓ^n	the Lebesgue measure on $\mathbb{R}^n$;
$\mathcal{B}(X)$	the Borel σ-algebra on X;
$\mathcal{B}_0(X)$	the bounded Borel σ-algebra on X;
$\mathcal{B}^n$	the Borel σ-algebra on $\mathbb{R}^n$;
$\mathcal{B}_0^n$	the bounded Borel σ-algebra on $\mathbb{R}^n$.

Chapter I

Introduction

First and second-order characteristics are important and widely used to describe point patterns but may not describe the distribution completely: it might happen that processes with different distributions have the same characteristics.

For instance, Baddeley A.J. and Silverman B. built a model which have the same first and second-order characteristics as the Poisson process but strongly differs from it (see [3]). Thus, they introduced the so-called T-function, which is a third-order analogue to Ripley's K-function. It is defined as the expected number of r-close pairs of points in a r-ball centered at the typical point and is more sensitive to clustering than K.

Previously, Moller J., Syversveen A.R., Waagepetersen R.P. had already introduced a third-order characteristic, the z-function (see [5]), designed to distinguish between log-Gaussian Cox processes and other processes, better than second-order characteristics would do.

We examined in the present study trough simulations the behaviour of these two functions for various processes, how a change in parameters affected them, their usefulness in the description of the distribution of point patterns and if one of them was more successful in that task.

Chapter II

General theory and basic properties

This chapter presents the general theory of point processes. We will give numerous notations, definitions, theorems and examples we will need in the following chapters.

1. Introduction

We consider the complete separable metric space (X, d) for which any bounded closed set on it is compact. Given the definition of a locally finite measure, we define the measurable space $(M, \mathcal{M})$, where M is the family of all locally finite subsets of X (each bounded subset of X is finite) and $\mathcal{M}$ is the smallest σ-algebra on M such that any mapping $\varphi(B)$ for $B \in \mathcal{B}_0(X)$ is measurable. That is

$$M = \{\varphi \in X : \varphi(B) < +\infty, \text{ for any } B \in \mathcal{B}_0(X)\},$$
$$\mathcal{M} = \sigma\{\varphi \in M : \varphi(B) \text{ is measurable for any } B \in \mathcal{B}_0(X)\}.$$

Given a probability space (Ω, Σ, P), we define a *random measure* Φ on X as a measurable mapping from (Ω, Σ, P) to $(M, \mathcal{M})$.

The probability measure $Q_\Phi = P(\Phi^{-1})$ is called the *distribution* of the random measure Φ and the measure $\Lambda_\Phi(.) = \boldsymbol{E}\Phi(.)$ is its *intensity measure*.

2. Point process

We now define the measurable space $(N, \mathcal{N})$ which is a restriction of the previous space $(M, \mathcal{M})$ to measures taking only natural values,

$$N = \{\varphi \in X : \varphi(B) \in \mathbb{R} \setminus \{+\infty\} \cup \mathbb{N}, \text{ for any } B \in \mathcal{B}_0(X)\},$$
$$\mathcal{N} = \sigma\{\varphi \in N : \varphi(B) \text{ is measurable for any } B \in \mathcal{B}_0(X)\}.$$

A *point process* is a special case of a random measure. A point process Φ on $X = \mathbb{R}^d$ is a measurable mapping from (Ω, Σ, P) to $(N, \mathcal{N})$. It can be seen as a random measure counting the number of points lying in a subset of the set X. When writing Φ we understand the random closed set $\Phi = \{x_1, \ldots, x_n\}$ and $\Phi(B) = n$ indicates that the set $B \in \mathcal{B}_0(X)$ contains exactly n points of the point process Φ.

A point process being a random measure, it generates a distribution on $(N, \mathcal{N})$ and has an intensity measure. The *distribution* P of a point process Φ is determined by the probabilities

$$P(\Phi \in Y) = P(\{\omega \in \Omega : \Phi(\omega) \in Y\}) \text{ for } Y \in \mathcal{N}, \tag{II.1}$$

and its *intensity measure* Λ is defined by

$$\Lambda(B) = \boldsymbol{E}\,\Phi(B) = \boldsymbol{E} \sum_{x \in \Phi} 1_{[x \in B]} \text{ for } B \in \mathcal{B}. \tag{II.2}$$

We also define the *finite-dimensional distributions*, which are of the form

$$P(\Phi(B_1) = n_1, \ldots, \Phi(B_n) = n_n), \text{ where } B_i \in \mathcal{B}_0(X) \text{ and } n_i \in \mathbb{N} \text{ for any } i \in \mathbb{N}. \tag{II.3}$$

These are of particular important because the distribution of Φ on $(N, \mathcal{N})$ is uniquely determined by the system they generate for $n = 1,2,3, \ldots$
If we consider in addition in our definition of $(N\,\mathcal{N})$ that the subsets of X in N are also simple $(i \neq j \Rightarrow x_i \neq x_j)$, then the point process is *simple* and its distribution P can be determined by a smaller system, the system of *void probabilities* of the form

$$P(\Phi(K) = 0) = P(\{\varphi \in \boldsymbol{N} : \varphi(K) = 0\}), \text{ for all compact sets } K. \tag{II.4}$$

We say that a point process Φ is *stationary* (or equivalently its distribution) if every translation leaves its distribution unchanged, that is the processes Φ and $\Phi_{+x} = \{x_1 + x, \ldots, x_n + x\}$ have the same distribution for any $x \in X$. Using the previous definition (II.1), we have

$$P(\Phi \in Y) = P(\Phi_{+x} \in Y) \text{ for any } Y \in \mathcal{N} \text{ and any } x \in X.$$

Similarly, we say that a process is *isotropic* (or its distribution) if the distribution is unchanged under rotation about the origin.
For a process which is both stationary and isotropic, we speak of *motion invariance*. The notion of motion invariance is very useful as its simplifies calculus of a great number of statistics (sometimes stationarity is enough for simplifications).

3. Moment characteristics of a point process

The first, and very important, characteristic we see is the *intensity measure* or *first order moment measure* Λ of a point process Φ. It is the mean number of point in a set $B \in \mathcal{B}(X)$. We already gave a definition (see (II.2)) and just precise it for the case that the distribution of the process is P

$$\Lambda(B) = \int \varphi(B) P(d\varphi), \text{ for } B \in \mathcal{B}(X). \tag{II.5}$$

If we consider a stationary point process, the intensity measure is translation invariant and simplifies. The only locally finite measure that is translation invariant on $(\mathbb{R}^d, \mathcal{B}^d)$ being the Lebesgue measure $\ell(.)$ (up to a constant), we have for a point process Φ on $(\mathbb{R}^d, \mathcal{B}^d)$

$$\Lambda(B)=\lambda\,\ell^{d}(B),\ \text{for some constant}\ \lambda. \tag{II.6}$$

The constant λ defined above is called the *intensity* of the process Φ and may be infinite. It is the mean number of points of the process per unit volume (as one can see, if we take B with volume one).

Other important characteristics are the higher order moment measures. The n-th *order moment measure* $\mu^{(n)}$ of a point process Φ, for $n\in\mathbb{N}$ is the measure defined on $\mathcal{B}^{n}(X)$ by

$$\mu^{(n)}(B_1\times\ldots\times B_n)=\boldsymbol{E}\sum_{x_1,\ldots,x_n\in\Phi}1_{[x_1\in B_1,\ldots,x_n\in B_n]}=\boldsymbol{E}\left(\Phi(B_1)\ldots\Phi(B_n)\right), \tag{II.7}$$

for any $B_i\in\mathcal{B}^{d}$, $i\in\mathbb{N}$.

Moreover, for any non-negative function f on X^n holds

$$\begin{aligned}\boldsymbol{E}\sum_{x_1,\ldots,x_n\in\Phi}f(x_1,\ldots,x_n)&=\int\sum_{x_1,\ldots,x_n\in\varphi}f(x_1,\ldots,x_n)\;P(d\varphi)\\&=\int\int f(x_1,\ldots,x_n)\;\varphi\left(d(x_1,\ldots,x_n)\right)\;P(d\varphi)\\&=\int f(x_1,\ldots,x_n)\;\mu^{(n)}\left(d(x_1,\ldots,x_n)\right).\end{aligned} \tag{II.8}$$

We define the n-th *order factorial moment measure* $\alpha^{(n)}$ of a point process Φ, which is defined on $\mathcal{B}^{n}(X)$ for any $B_i\in\mathcal{B}^{d}$, $i\in\mathbb{N}$ by summing over n-tuples of distinct points

$$\alpha^{(n)}(B_1\times\ldots\times B_n)=\boldsymbol{E}\sum_{x_1,\ldots,x_n\in\Phi}^{\neq}1_{[x_1\in B_1,\ldots,x_n\in B_n]}\ . \tag{II.9}$$

For $B_1,\ldots,B_n$ pairwise disjoint sets, no point is counted more than once, and then

$$\mu^{(n)}(B_1\times\ldots\times B_n)=\alpha^{(n)}(B_1\times\ldots\times B_n). \tag{II.10}$$

Again, for every non-negative function f on X^n we have

$$\begin{aligned}\boldsymbol{E}\sum_{x_1,\ldots,x_n\in\Phi}^{\neq}f(x_1,\ldots,x_n)&=\int\sum_{x_1,\ldots,x_n\in\varphi}^{\neq}f(x_1,\ldots,x_n)\;P(d\varphi)\\&=\int f(x_1,\ldots,x_n)\;\alpha^{(n)}\left(d(x_1,\ldots,x_n)\right).\end{aligned} \tag{II.11}$$

For $n=1$, we have $\mu^{(1)}(B)=\alpha^{(1)}(B)=\Lambda(B)$.

If the process Φ is stationary we get $\mu^{(1)}(.)=\alpha^{(1)}(.)=\lambda\,\ell^{d}(.)$. (II.12)

For a factorial moment measure $\alpha^{(n)}$ absolutely continuous with respect to the Lebesgue measure ℓ^{n} on X^n, there exists a density $\rho^{(n)}$ such that for any strictly positive bounded measurable function f on X^n holds

$$\boldsymbol{E} \sum_{x_1,\dots,x_n\in\Phi}^{\neq} f(x_1,\dots,x_n) = \int f(x_1,\dots,x_n)\,\alpha^{(n)}\big(d(x_1,\dots,x_n)\big) = \int f(x_1,\dots,x_n)\,\rho^{(n)}(x_1,\dots,x_n)\,dx_1\dots dx_n. \tag{II.13}$$

Such densities are called n-th *order product densities*. Combining (II.10) and (II.13) leads to

$$\mu^{(n)}(B_1\times\dots\times B_n) = \int_{B_1}\dots\int_{B_n}\rho^{(n)}(x_1,\dots,x_n)\,dx_1\dots dx_n, \tag{II.14}$$

for pairwise disjoint $B_1,\dots,B_n$.

From (II.12), we see that for a stationary point process holds $\rho^{(1)}=\rho=\lambda$.

4. Campbell measure

A point process Φ is, as we have seen before, nothing else but a random measure on $X=\mathbb{R}^d$. Thus (see Chapter V), such a process, with distribution P, has a *Campbell measure* C.
C is defined on $(\mathbb{R}^d\times N, \mathcal{B}^d\times\mathcal{N})$ and satisfies

$$\int\sum_{x\in\varphi} f(x,\varphi)\,P(d\varphi) = \int f(x,\varphi)\,C\big(d(x,\varphi)\big), \tag{II.15}$$

for any non-negative measurable function f on $\mathbb{R}^d\times N$. For $B\in\mathcal{B}^d$ and $Y\in\mathcal{N}$, we can also write

$$C(B\times Y) = \int \varphi(B)\,1_{[\varphi\in Y]}\,P(d\varphi) = \boldsymbol{E}[\Phi(B)\colon \Phi\in Y].$$

The *reduced Campbell measure* is defined by

$$\int\sum_{x\in\varphi} f(x,\varphi\setminus\{x\})\,P(d\varphi) = \int f(x,\varphi)\,C^!\big(d(x,\varphi)\big). \tag{II.16}$$

5. Palm distribution

A point process Φ also has its *Palm distribution*: it is the density of the Campbell measure C of the process with respect to the intensity measure Λ (again, see Chapter V). The Palm distribution P_x at x (or with respect to the point x) satisfies

$$C(B\times Y) = \int_B P_x(Y)\,\Lambda(dx), \text{ for } B\in\mathcal{B}^d \text{ and } Y\in\mathcal{N}. \tag{II.17}$$

The Palm distribution of a point process can be interpreted as the distribution of the process conditional on x being a point of the process (the process has a point at x).
In the stationary case for a point process with positive finite intensity λ, we can write

$$C(B\times Y)=\lambda\int_B P_x(Y)\,dx. \tag{II.18}$$

Stationarity also implies $P_0(Y)=P_x(Y)$, the Palm distribution at the origin is the same as the one at any point x. This is due to the fact that the process being stationary, the Campbell measures $C(B\times Y)$ and $C(B\times Y_{+x})$ are equal and so, in terms of integrals, that means $\lambda\int_B P_z(Y)\,dz=\lambda\int_B P_y(Y_{+x})\,dy=\lambda\int_B P_{y-x}(Y)\,dy$. This is $P_z(Y)=P_{z-x}$. Taking $z=0$ gives the result.

Similarly, the *reduced Palm distribution* is defined by $C^!(B\times Y)=\int_B P_x^!(Y)\,\Lambda(dx)$. (II.19)

6. Other characteristics

One important function is the *pair correlation function* $g(x,y)$. It will be used later on to define the z-function in Chapter III. It is of the form

$$g(x,y)=\frac{\rho^{(2)}(x,y)}{\rho^{(1)}(x)\rho^{(1)}(y)}, \text{ for } (x,y)\in(\mathbb{R}^d)^2. \tag{II.20}$$

For a process which satisfies the condition of movement invariance, the function depends just on the distance between the points. We have $\rho^{(2)}(x,y)=\rho^{(2)}(x-y,0)=\rho^{(2)}(\|x-y\|)$ we can write

$$g(r)=\frac{\rho^{(2)}(r)}{\lambda^2}, \text{ with } r=\|x-y\|. \tag{II.21}$$

Under the same assertions of movement invariance (although stationarity is sufficient for the present definition, we consider also isotropy which will be necessary for the next ones), we can introduce the *second reduced moment measure* $\mathcal{K}$. It is defined as the mean measure of the point process Φ with respect to the reduced Palm distribution at the origin $P_0^!$ divided by the intensity λ. Let us note $\boldsymbol{E}_0^!$ the expectation with respect to $P_0^!$, then it is defined by

$$\mathcal{K}(B)=\frac{1}{\lambda}\boldsymbol{E}_0^!\Phi(B)=\frac{1}{\lambda}\int\varphi(B)\;P_0^!(d\varphi)=\frac{1}{\lambda}\int\varphi(B\setminus\{0\})\;P_0(d\varphi), \text{ for } B\in\mathcal{B}^d. \tag{II.22}$$

If the second order product density $\rho^{(2)}$ exists, we have the following relation between this density and the second order moment measure $\mathcal{K}$

$$\mathcal{K}(B)=\frac{1}{\lambda^2}\int_B\rho^{(2)}(r)\,dr, \text{ for } B\in\mathcal{B}^d. \tag{II.23}$$

From (II.21) we see that the pair correlation function g is the density of the second reduced factorial moment measure $\mathcal{K}$ with respect to the Lebesgue measure.

Definition of $\mathcal{K}$ leads to the definition of the *second reduced moment function* K or *Ripley's K-function* and also to the definition of the *L-function*. For any $r\geq 0$ let us define

$$K(r)=\mathcal{K}\left(b(0,r)\right), \tag{II.24}$$

$$L(r)=\sqrt[d]{\frac{K(r)}{\omega_d}}, \tag{II.25}$$

where ω_d is the volume of the unit ball. $\lambda K(r)$ is the mean number of points of the process Φ which lie in the r-ball centered at the typical point (which is not counted).

We additionally introduce the *spherical contact distribution function* $F(r)$ of any point process Φ which is defined by

$$F(r)=P\left(\Phi(b(0,r))>0\right), \text{ for } r\geq 0. \tag{II.26}$$

and when the process is stationary, the *nearest neighbour distance distribution function* $G(r)$ or *distribution function of the distance from the typical point of* Φ *to its nearest neighbour*

$$G(r)=P_0^!\left(\varphi\in N:\varphi\left(b(0,r)\right)>0\right), \text{ for } r\geq 0. \tag{II.27}$$

Combining (II.26) and (II.27) we introduce a last characteristic, the J-function, of the form

$$J(r)=\frac{1-G(r)}{1-F(r)}, \text{ for } r\geq 0. \tag{II.28}$$

7. Statistics for planar point process

We give here a brief description of the estimators for the characteristics λ and K we introduced previously. Statistical analysis is often based on observing one realization (a sample) of a point process Φ in a bounded window W. To simplify our study, we will consider that the processes are motion invariant and simple.
The major problem we have to face is that of edge-effect when we need information about the neighbourhood of the typical point; when a point lies too close to the boundaries of the window W such information may not be available. This is the reason why edge-corrections where introduced: to obtain unbiased estimators. Some of them are simple, such as the ones based on minus-sampling, some others have a much more complicated form and use weight functions.

The first estimator we introduce is the estimator of the intensity. For a motion invariant point process Φ with intensity λ in a bounded window W, it is defined by

$$\hat{\lambda}=\frac{\Phi(W)}{\ell^d(W)}. \tag{II.29}$$

We see, using definition (II.2) and formula (II.6), that this estimator is unbiased.

To define other statistics, we make use of the Campbell-Mecke theorem (see (V.13-V.14)). The definition of the second reduced moment measure $\mathcal{K}(r)$ (II.22), the definition of the second reduced moment function $K(r)$ (II.24) lead to the following for $K(r)$

$$\lambda K(r) = \boldsymbol{E}_{\mathbf{0}}^{!}\Phi\big(b(0,r)\big) = \boldsymbol{E}\sum_{x,0\in\Phi} 1_{[x\in b(0,r)\setminus\{0\}]} = \boldsymbol{E}\sum_{x,\,y\in\Phi} 1_{[x\in b(y,r)\setminus\{y\}]} \quad . \tag{II.30}$$

When observing the process in a bounded window W we get

$$\lambda K(r) = \frac{\boldsymbol{E}\sum_{x,\,y\in\Phi\cap W} 1_{[x\in b(y,r)]}}{\boldsymbol{E}\sum_{x\in\Phi} 1_{[x\in W]}} = \frac{\boldsymbol{E}\sum_{x,\,y\in\Phi\cap W} 1_{[x\in b(y,r)]}}{\boldsymbol{E}\,\Phi(W)} = \frac{\boldsymbol{E}\sum_{x,\,y\in\Phi\cap W} 1_{[0<\|x-y\|\le r]}}{\lambda\,\ell^{d}(W)} \quad . \tag{II.31}$$

This formula is the base for the construction of estimators for the function $K(r)$ by first estimating $\lambda^2 K(r)$.

The following estimator uses the method of minus-sampling: each point included in the estimation procedure has to lie at a distance at least r from the borders of the window W. Let us note $W_{-b(0,r)}$ the window eroded by r, then a natural estimator for $\lambda^2 K(r)$ is

$$\widehat{\lambda^2 K_b(r)} = \frac{\sum_{x\in\Phi\cap W_{-b(0,r)},\,y\in\Phi\cap W} 1_{[0<\|x-y\|\le r]}}{\ell^{d}(W_{-b(0,r)})} \quad . \tag{II.32}$$

The estimator is unbiased as we can see from (II.31).

Another estimator for $\lambda^2 K(r)$ is of the form

$$\widehat{\lambda^2 K_t(r)} = \sum_{x,\,y\in\Phi\cap W} \frac{1_{[0<\|x-y\|\le r]}}{\ell^{d}(W_x\cap W_y)}, \tag{II.33}$$

where W_x stands for the translated window.

The definition is correct when $\ell^{d}(W_x\cap W_y)>0$, for x, y such that $0\le\|x-y\|\le r$. For a square observation window, this is always true as soon as the side of the window is greater than r.
This estimator is also unbiased. To prove this assertion we first rewrite our definition

$$\widehat{\lambda^2 K_t(r)} = \sum_{x,\,y\in\Phi}^{\neq} \frac{1_{[\|x-y\|\le r]}\,1_{[x\in W]}\,1_{[y\in W]}}{\ell^{d}(W_x\cap W_y)}.$$

We now apply $\boldsymbol{E}$ and use definitions (II.13), (II.21) and (II.23) to obtain the result

$$\begin{aligned}
\boldsymbol{E}\,\widehat{\lambda^2 K_t(r)} &= \int \frac{1_{[0<\|x-y\|\le r]}\,1_{[x\in W]}\,1_{[y\in W]}}{\ell^{d}(W_x\cap W_y)}\,\alpha^{(2)}\big(d(x,y)\big) \\
&= \lambda^2 \int\int f(x,y)\,\frac{\rho^2(x,y)}{\lambda^2}\,dx\,dy \\
&= \lambda^2 \int\int f(x,x+h)\,\frac{\rho^2(h)}{\lambda^2}\,dx\,dh \\
&= \lambda^2 \int 1_{[\|h\|\le r]}\,\frac{\rho^2(h)}{\lambda^2}\,dh
\end{aligned}$$

$$= \lambda^2 K(r).$$

We finally introduce a last estimator for $\widehat{\lambda^2 K(r)}$, which is the one Ripley B.D. introduced (see [11]), and which is of the following form

$$\widehat{\lambda^2 K_i(r)} = \sum_{x,y \in \Phi \cap W} \frac{1_{[0<\|x-y\| \le r]}}{\ell^d(W)} \frac{2\pi \|x-y\|}{\partial b(X, \|x-y\|) \cap W} \quad . \tag{II.34}$$

It is based on the ratio of angles of the arcs in the window W of a circle with centre x and radius $\|x-y\|$. The estimator is unbiased for

$$r \le \{s : \exists x \in W \text{ such that } \partial b(x,s) \text{ is not completely outside of the window } W\}.$$

Many other estimators have been introduced. The curious reader can refer for example to Baddeley A.J., Gill R.D. [2] a Ohser J. [7].

The function $K(r)$ being of greater interest than $\lambda^2 K(r)$, we usually divide the previous estimators by $\widehat{\lambda^2} = \frac{\Phi(W)^2 - \Phi(W)}{(\ell^d(W))^2}$ which is an unbiased estimator for λ^2 in the case of a Poisson process (this is generally not true for other processes). That leads to ratio-unbiased estimators for $K(r)$ (in the Poisson case).

8. Examples of point processes

a) Binomial point process

The simplest point process that could be is a point process Φ with one random point which is uniformly distributed in $W \subset \mathbb{R}^d$ compact (hence bounded). Such a point process has a distribution of the form

$$P(x \in B) = \frac{\ell^d(B)}{\ell^d(W)}, \text{ for } B \in \mathcal{B}^d,\ B \subset W. \tag{II.35}$$

A point process Φ_B that is the superposition of n independent uniformly distributed random points is called a *binomial point process of* n *points*. Its distribution is defined by

$$P(x_1 \in B_1, \ldots, x_n \in B_n) = \prod_{i=1}^{n} P(x_i \in B_i) = \frac{1}{\left(\ell^d(W)\right)^n} \prod_{i=1}^{n} \ell^d(B_i) \text{ , for } B_i \in \mathcal{B}^d, B_i \subset W. \tag{II.36}$$

For a binomial point process Φ_B, the finite-dimensional distributions of the process are given by

$$P\left(\Phi_B(B_1) = n_1, \ldots, \Phi_B(B_n) = n_n\right) = \frac{n!}{n_1! \ldots n_n!} \cdot \frac{1}{\left(\ell^d(W)\right)^n} \cdot \prod_{i=1}^{n} \ell^d(B_i)^{n_i},$$

for any $B_1, \ldots, B_n \in \mathcal{B}^d$ disjoint sets such that $\cup B_i = W$ and $n_1 + \ldots + n_n = n$ and the void

probabilities by

$$\frac{\left(\ell^d(W)-\ell^d(K)\right)^n}{\left(\ell^d(W)\right)^n}, \text{ for any } K\subset W \text{ compact.}$$

b) Poisson point process

This is for sure the most important point process. It describes complete randomness and though is not often used to represent natural models, it is used to construct more complicated point processes that are useful when we want to do so.

Such a point process is completely characterized by its intensity measure. A *Poisson point process* Φ_P with intensity measure Λ_P is a process that satisfies the two following properties

$$\begin{cases} \_ \text{ the number of points of the process in } B\in\mathcal{B}_0^d \text{ is Poisson distributed with mean } \Lambda_P(B): \\ \qquad P(\Phi_P(B)=n)=\left(\Lambda_P(B)\right)^n\frac{\exp\left(-\Lambda_P(B)\right)}{n!} \\ \_ \text{ the numbers of points } \Phi_P(B_1)\dots\Phi_P(B_n) \text{ in } B_1,\dots,B_n\in\mathcal{B}^d \text{ pairwise disjoint are independent.} \end{cases}$$

The void probabilities are of the form $\exp\left(-\Lambda_P(B)\right)$ for $B\in\mathcal{B}_0^d$ and for disjoint $B_1,\dots,B_n\in\mathcal{B}_0^d$ the finite-dimensional distribution of the form

$$P\left(\Phi_P(B_1)=n_1,\dots,\Phi_P(B_n)=n_n\right)=\prod_{i=1}^{n}\left(\Lambda_P(B_i)\right)^{n_i}\frac{\exp\left(-\Lambda_P(B_i)\right)}{n_i!}.$$

The n-th order factorial moment measure are $\alpha_P^{(n)}(B_1\times\dots\times B_n)=\Lambda_P(B_1)\dots\Lambda_P(B_n)$.

If it exists, the density λ of $\Lambda_P(B)$ with respect to the Lebesgue measure is called the *intensity function* of the process Φ_P. In such a case, the n-th order product densities are given by

$$\rho^{(n)}(x_1,\dots,x_n)=\lambda(x_1)\dots\lambda(x_n). \tag{II.37}$$

We should notice that the Poisson point process is in general not stationary. Should it be stationary, then $\lambda(x)=\lambda$ is constant and we just call it the *intensity* of the process. Then, the n-th order product densities can be simply expressed by

$$\rho^{(n)}(x_1,\dots,x_n)=\lambda^n. \tag{II.38}$$

Thus, by definitions (II.20) and (II.23), the pair correlation function $g(x,y)$ of a Poisson point process Φ_P is equal to 1 for any pair of points in $(\mathbb{R}^d)^2$ and its $K-$function is $\int_{b(0,r)}dr=\omega_d r^d$, for $r\geq 0$. This implies $L(r)=r$.

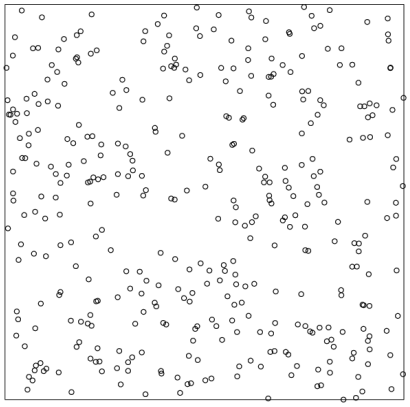

Fig. II.1: realization of a stationary Poisson point process with intensity 400.

For motion invariant processes, when the pair correlation function $g(r)$ is greater than one, it indicates a frequent inter-point distance equals to r. On the opposite, small values indicate inhibition (only a few points lie at a distance r from another point).

c) Cox processes

Let us consider that the intensity measure of the Poisson process Φ_P is the realization of a random measure Ψ_P that generates the distribution Q_{Ψ_P} on $(N, \mathcal{N})$. The resulting process which is Poisson with intensity Ψ_P conditional on the realization of the random intensity measure $\Psi_P = \psi_P$, is called a *Cox process*. If the measure Ψ_P is no more random but deterministic, the process is a simple Poisson process.

We consider a Poisson process that generates the distribution Q_P and has the intensity measure Λ_P in addition to the random measure Ψ_P and its distribution Q_{Ψ_P}. Properties of a Cox process Φ_C with driving random measure Ψ_P directly follow from the properties of the process $\Phi_C | \Psi_P = \psi_P$ which is Poisson.

Its distribution is of the form

$$P_C(Y) = \int Q_P(Y) Q_{\Psi_P}(d\,\Lambda_P), \text{ for } Y \in \mathcal{N}. \tag{II.39}$$

Using (II.39), the void probabilities of the process have the following form

$$\int \exp\left(-\Lambda_P(K)\right) Q_{\Psi_P} d(\Lambda_P) \quad \text{or equivalently} \quad \boldsymbol{E} \exp\left(-\Lambda_P(K)\right), \text{ for } K \text{ compact.} \tag{II.40}$$

If we denote Λ_{Ψ_P} the intensity measure of Ψ_P, the intensity measure Λ_C of Φ_C is

$$\Lambda_C(B) = \Lambda_{\Psi_P}(B), \text{ for any } B \in \mathcal{B}^d. \tag{II.41}$$

To prove this, we use the definition (II.39) we gave for the distribution and Fubini's theorem

$$\begin{aligned}\Lambda_C(.) = \boldsymbol{E}\,\Phi_C(.) &= \int \mu(.)\, P_C(d\,\mu) \\ &= \int\int \mu(.) Q_P(d\,\mu)\; Q_{\Psi_P}(d\,\Lambda_P) \\ &= \int \boldsymbol{E}\,\Phi_P(.)\; Q_{\Psi_P}(d\,\Lambda_P) \\ &= \int \Lambda_P(.)\; Q_{\Psi_P}(d\,\Lambda_P) \\ &= \boldsymbol{E}\,\Psi_P(.) = \Lambda_{\Psi_P}(.).\end{aligned}$$

The Cox process has the same intensity measure as its driving random measure Ψ_P. If the random measure is stationary, so is the Cox process Φ_C and they have the same intensity function.

d) Log-Gaussian Cox processes

Log-Gaussian process Φ_{LGC} is a special case of Cox process when the intensity measure is log-Gaussian.
In other words, the logarithm of the density ψ_P of the measure Ψ_P is Gaussian. That is
$\psi_P(s) = \exp\big(Y(s)\big)$, where $Y = \{Y(s) : s \in \mathbb{R}^2\}$ is a Gaussian process on $\mathbb{R}^2$.

We will assume on the following that Ψ_P is motion invariant, thus the log-Gaussian process will also be. We also assume the process is simple. We already know that for such a process, distribution is completely characterized by void probabilities (given here by (II.40)). Log-Gaussian process is completely characterized by the intensity and the pair-correlation of Ψ_P (alternatively by the intensity $\mu = \boldsymbol{E}\,Y(s)$ and pair correlation $r(s_1 - s_2) = \dfrac{\boldsymbol{cov}\big(Y(s_1), Y(s_2)\big)}{\sigma^2}$ of Y). In order for the random measure to be well defined for $B \in \mathcal{B}_0^d$, we have to impose the following two conditions

$$\begin{cases} \_ \text{ the realizations of } \Psi_P \text{ are integrable almost surely;} \\ \_ \text{ the measure } \Psi_P \text{ is uniquely determined: we will here consider that it is a continuous} \\ \quad \text{modification of } Y. \end{cases}$$

A log-Gaussian Cox process Φ_{LGC} is stationary iff the Gaussian process Y is stationary. For such a point process, the n-th order product density $\rho^{(n)}$ is

$$\rho^{(n)}(s_1, \ldots, s_n) = \exp\left(n\,\mu + \sigma^2\left(\frac{n}{2} + \sum_{1 \le i < j \le n} r(s_i - s_j)\right)\right) = \rho^n \prod_{1 \le i < j \le n} g(s_i - s_j). \qquad \text{(II.42)}$$

In particular,

$$\begin{cases} \lambda = \rho = \rho^{(1)}(s) = \exp\left(\mu + \dfrac{\sigma^2}{2}\right) \text{ is the intensity of } \Phi_{LGC}, \\ g(s_1 - s_2) = \dfrac{\rho^{(2)}(s_1, s_2)}{\lambda^2} = \exp\big(\sigma^2\, r(s_1 - s_2)\big) \text{ is the pair correlation function of } \Phi_{LGC}. \end{cases} \qquad \text{(II.43)}$$

To prove the assertion, we remember that $\sum_{i=1}^{n} Y(s_i) \sim \mathcal{N}(E, V)$ with $E = \sum_{i=1}^{n} \mu(s_i) = n\mu$ and $V = \sum_{i=1}^{n} \sigma^2 + 2 \sum_{1 \le i < j \le n} \sigma(s_i)\sigma(s_j) r(s_i, s_j) = \sigma^2 \left(n + 2 \sum_{1 \le i < j \le n} r(s_i, s_j) \right)$ (see [1]).

The n-th order product density is defined as

$$\rho^{(n)}(s_1, \ldots, s_n) = \boldsymbol{E} \prod_{i=1}^{n} \Psi_P(s_i) = \boldsymbol{E} \prod_{i=1}^{n} \exp\left(Y(s_i)\right) = \boldsymbol{E} \exp\left(\sum_{i=1}^{n} Y(s_i) \right) = \exp\left(E + \frac{V}{2} \right). \quad \text{(II.44)}$$

We deduce from (II.44) the form of the first and second order product densities and get the final result using (II.20) for the pair correlation function g.

e) Operations on point processes

To construct other point processes we can use the previous point processes described above and apply several operations. We introduce here the principal operations used to construct new models. The easiest operation is *superposition*. We consider two point processes Φ_1 and Φ_2 generated respectively by the distributions P_1 and P_2 on $(N, \mathcal{N})$. We assume that there is no common point, $\Phi_1 \cap \Phi_2 = \emptyset$ almost surely. Then superposition gives the following process $\Phi_{sp} = \Phi_1 \cup \Phi_2$.

From the definition of the process, we deduce that the intensity measure is of the form

$$\Lambda_{sp} = \Lambda_1 + \Lambda_2, \quad \text{(II.45)}$$

and when the processes are stationary

$$\lambda_{sp} = \lambda_1 + \lambda_2, \quad \text{(II.46)}$$

and when the processes are independent, the distribution is

$$P_{sp} = P_1 * P_2, \quad \text{(II.47)}$$

where $*$ denotes the convolution of measures.

Clustering consists in replacing each point x_i of a point process Φ by a cluster of points N_{x_i}, which is also a point process. We assume that the number of points in the clusters is almost surely finite and that the clusters do not have common points, that is $N_x \cap N_y = \emptyset$ almost surely if $x \neq y$. The resulting process is the cluster point process $\Phi_{cl} = \cup N_{x_i}$, for $x_i \in \Phi$.

Considering the parent point process Φ is stationary and the N_i are iid clusters with distribution P_{cl} independent of the parent point, we have homogeneous independent clustering. The intensity λ_{cl} of the process Φ_{cl} is given by

$$\lambda_{cl} = \lambda \bar{N}(.), \quad \text{(II.48)}$$

where $\bar{N}(.)=\int \varphi(.)\, P_{cl}(d\varphi)$ is the mean number of point in a finite point set of distribtution P_{Cl} and λ is the intensity of Φ.

To conclude this part on the operations on point processes, we introduce *thinning*. Thinning consists in deleting points according to a certain rule. If the deletion of a certain point is independent of the other points of the process we speak of independent thinning. In the other cases, we say dependent thinning. The simplest method is called p-thinning and consists in deleting points with probability p and retaining them with probability $1-p$. The method of $p(x)$-thinning depends on the location of the point x.

We can infer the properties of the thinned process Φ_{th} from these of the original process Φ. For $p(x)$-thinning, the intensity measure is

$$\Lambda_{th}(.)=\int p(x)1_{[x\in.]}\,\Lambda(dx), \text{ where } \Lambda \text{ is the intensity measure of } \Phi. \qquad \text{(II.49)}$$

We know from (II.2) that

$$\Lambda_{th}(.)=\boldsymbol{E}\sum_{x\in\Phi_{th}} 1_{[x\in.]}=\boldsymbol{E}\sum_{x\in\Phi} 1_{[x\in.]}\,p(x).$$

We infer the formula using (II.8).

When we use p-thinning on a stationary point process, then the resulting process Φ_{th} is also stationary and its intensity is $\lambda_{th}=\lambda p$, with λ the intensity of Φ.

f) Poisson Cluster process

A simple example of a cluster point process. Parents are distributed according to a homogeneous Poisson process Φ_P with points x_{Pi} and intensity λ. Each parent point x_{Pi} generates a cluster N_{Ci} which is finite and forms a family of independent and identically distributed points that are independent of the parent point process Φ_P. The resulting process Φ consists in the union of the clusters, $\Phi=\cup N_{Ci}$.

If the points in a cluster have distribution P_{Cl} and mean number of points per cluster ϖ, then the intensity of the Poisson cluster process Φ is

$$\lambda_{PC}=\lambda\varpi. \qquad \text{(II.50)}$$

g) Neymann-Scott processes

This is an other example of cluster process: we apply independent clustering to a stationary Poisson point process. The parent process is stationary Poisson with intensity λ, the clusters N_x are formed of a random number of points that are independent and identically distributed about the parent point. In the resulting process we only consider the daughter points; the parents are not included. It is called a *Neymann-Scott process* and is under the previous assumptions stationary.

Such a process has intensity

$$\lambda_{NS}=\lambda\,\lambda_{cl}, \tag{II.51}$$

and pair correlation function

$$g(x,y)=1+\frac{1}{\lambda}\int p(t)\,p(x-y+t)\,dt, \tag{II.52}$$

where the integral is the density of the difference $x-y$ for two independent points x, y which have the same density p (see Moller J., Waagepetersen R.P. [6] for more details).

The *Matérn cluster process* is a special case of Neymann-Scott process which is also a Cox process, the number of points in clusters given the parent process is restricted to be also Poisson.

We first generate a stationary Poisson process Φ_P with intensity $\lambda_{P_1}>0$. Then each point x in the parent process is replaced by a cluster N_x; the points of N_x are independent and uniformly distributed on $b(x,r)$, with r being a parameter of the model. The number of points in the representative cluster has Poisson distribution with parameter λ_{P_2}. The process has three parameters: intensities λ_{P_1}, λ_{P_2} and radius r.

Following definition (II.51), the Matérn's cluster process defined above has intensity

$$\lambda_{M.Cl}=\lambda_{P_1}\lambda_{P_2}, \tag{II.53}$$

and the function p introduced in (II.52) is equal to $\frac{1}{\pi r^2}$ on the ball $b(x,r)$, for $x\in\Phi_P$ and is 0 everywhere else (see [1]).

Thus, the pair correlation function is

$$g(\|x-y\|)=1+\frac{2}{\lambda_{P_1}\pi^2 r^2}\cdot\left(\arccos\left(\frac{\|x-y\|}{2\mathrm{r}}\right)-\frac{\|x-y\|}{2\mathrm{r}}\sqrt{1-\left(\frac{\|x-y\|}{2\mathrm{r}}\right)^2}\right),\ \text{for}\ \|x-y\|\le 2\mathrm{r} \tag{II.54}$$

and is 1 when the inter-point distance is greater.

To prove the assertion, we replace p by its value and integrate

$$\begin{aligned}\int p(t)\,p(x-y+t)\,dy&=\int\frac{1_{[\|y\|\le r]}}{\pi r^2}\cdot\frac{1_{[\|x-y\|\le r]}}{\pi r^2}\,dy\\&=\frac{1}{\pi^2 r^4}\,\ell^2\big(b(o,r)\cap b(x,r)\big)\\&=\frac{1}{\pi^2 r^4}\left[2\mathrm{r}^2\left(\arccos\left(\frac{\|x-y\|}{2\mathrm{r}}\right)-\frac{\|x-y\|}{2\mathrm{r}}\sqrt{1-\left(\frac{\|x-y\|}{2\mathrm{r}}\right)^2}\right)\right].\end{aligned} \tag{II.55}$$

Combining (II.52) and (II.55) leads to the result.

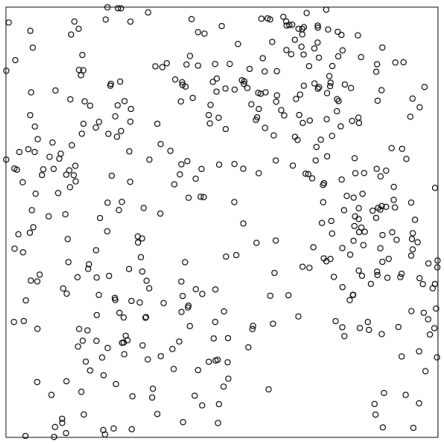

Fig. II.2: a realization of a Matérn cluster point process: the parent process has stationary Poisson distribution with intensity 33; the number of points in a cluster has stationary Poisson distribution with intensity 13; in each cluster, the points are independent and have uniform distribution on a ball with radius 0,2.

The *Thomas process* is an other special case but this time, the points in the clusters have normal distribution $\mathcal{N}(0,\sigma^2 Id_2)$. That is, the function p is of the form $p(x)=\frac{1}{2\pi\sigma^2}\exp\left(\frac{-\|x\|^2}{2\sigma^2}\right)$ (see again [1]). The Thomas process also has three parameters which are the intensities λ_{P_1}, λ_{P_2} and the variation σ^2. The intensity is again given by

$$\lambda_{Thom}=\lambda_{P_1}\lambda_{P_2}, \tag{II.56}$$

and the pair correlation function is

$$g(\|x-y\|)=1+\frac{1}{4\lambda_{P_1}\pi\sigma^2}\exp\left(\frac{-\|x-y\|^2}{4\sigma^2}\right). \tag{II.57}$$

Again, to prove (II.57) we write

$$\begin{aligned}\int p(t)\,p(x-y+t)\,dt &= \int \frac{1}{2\pi\sigma^2}\cdot\frac{1}{2\pi\sigma^2}\exp\left(\frac{-\|t\|^2}{2\sigma^2}\right)\exp\left(\frac{-\|(x-y)+t\|^2}{2\sigma^2}\right)dt\\ &= \frac{1}{4\pi^2\sigma^4}\int \exp\left(\frac{-\left(t^2+\left((x-y)+t\right)^2\right)}{2\sigma^2}\right)dt\\ &= \frac{1}{4\pi^2\sigma^4}\int \exp\left(\frac{-\left(t^2+(x-y)^2+t^2\pm 2(x-y)t\right)}{2\sigma^2}\right)dt\\ &= \frac{1}{4\pi^2\sigma^4}\int \exp\left(\frac{-\left(2t^2\pm 2(x-y)t+(x-y)^2\right)}{2\sigma^2}\right)dt\end{aligned}$$

$$= \frac{1}{4\pi^2\sigma^4} \int \exp\left(\frac{-\left(\left(t \pm \frac{x-y}{2} \right)^2 - \left(\frac{(x-y)}{2} \right)^2 + \frac{(x-y)^2}{2} \right)}{\sigma^2} \right) dt$$

$$= \frac{1}{4\pi^2\sigma^4} \exp\left(\frac{-\|x-y\|^2}{4\sigma^2} \right) \int \exp\left(\frac{-\left(t \pm \frac{x-y}{2} \right)^2}{\sigma^2} \right) dt .$$

We just have to calculate the integral for $t \in \mathbb{R}^2$.

We first remark that $\left\| t \pm \frac{x-y}{2} \right\|^2 = \left(t_1 \pm \frac{x_1-y_1}{2} \right)^2 + \left(t_2 \pm \frac{x_2-y_2}{2} \right)^2$, so the result is the square of the integral for $t \in \mathbb{R}$. We provide the transformation $u = \left(t \pm \frac{x-y}{2} \right) \frac{1}{\sigma}$ and make use of the Gauss integral $\int \sigma \ \exp\left(-u^2\right) du = \sqrt{\pi}\,\sigma$ to get the result.

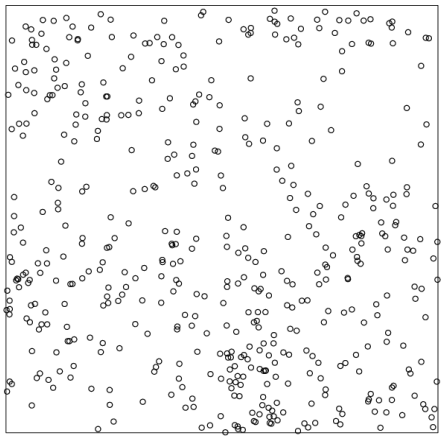

Fig. II.3: A sample of a Thomas point process: the parent process is stationary Poisson with intensity 33; the number of points in each cluster has stationary Poisson distribution with intensity 13; the points of the clusters have normal distribution with variation 0,08.

A last subclass of Neymann-Scott processes is formed by the *Gauss-Poisson processes*. In this example, each cluster consists of one or two points only with probability p_1 or $p_2 = 1 - p_1$ respectively. With probability p_1 we replace the parent point by a point at the same place (just like if we had kept the parent point). With probability p_2 the parent point is replaced by a cluster which has isotropic distribution and is composed of two points separated by a distance d (parameter of the process) and midpoint the parent point.

h) Hard-core point processes

This is an example of a thinned process. In a *hard-core point process*, points must not lie closer than a certain distance to an other point of the process.

We first generate a stationary Poisson point process with intensity λ and then erase the points of the process which do not fulfill conditions. Matérn hard-core processes of type I and II defined respectively by

$$\begin{cases} \Phi_{MatI} = \{x \in \Phi : \|x - y\| > r, \text{ for any } y \in \Phi, y \neq x\} \\ \Phi_{MatII} = \{x \in \Phi : m(x) < m(y) \text{ for any } y \in \Phi \cap b(x, r)\} \end{cases}$$

are of this kind. In type II, it is common to take m as a mark that indicates the arrival time: we erase a point if it lies close enough to an other one which was there earlier in time. Both of them are based on dependent thinning.

They are stationary and they respectively have intensity equal to

$$\lambda_{MatI} = \lambda \exp\left(-\lambda \omega_d r^d\right) \text{ and } \lambda_{MatII} = \frac{1 - \exp\left(-\lambda \omega_d r^d\right)}{\omega_d r^d} . \qquad \text{(II.58)}$$

The intensity of the MatérnII is higher than the intensity of the MatérnI; in the first case we proceed to deletion not only depending on the inter-point distance but also depending on the arrival time, thus we don't erase as many point as in the last. Realizations of these processes can be seen in *Fig. II.5* for the same intensity λ of the Poisson process and the same inhibition distance r.

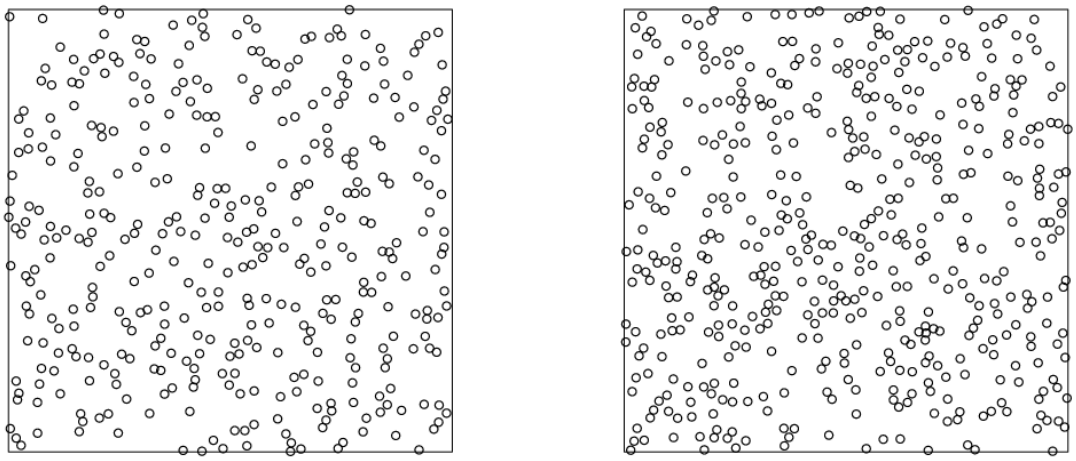

Fig. II.4: samples of MatérnI and MatérnII hard-core processes. Left: MatérnI hard-core process with intensity of the Poisson process 600 and inhibition distance 0,015. Right: MatérnII hard-core process with the same parameters as for the MatérnI.

Chapter III

T-function and z-function

1. Definition and properties of the T-function

The T-function was introduced by Schladitz K. and Baddeley A.J. in [11]. Let us consider Φ a point process defined on $(\mathbb{R}^d, \|.\|)$ and taking values in the measurable space $(N, \mathcal{N})$. To simplify our study, we will always assume that the process Φ is simple and stationary with intensity λ.

The T-function associated with the process Φ is defined as follows

$$T(r)=\frac{1}{2*\lambda^2}\boldsymbol{E}_{\mathbf{0}}^{!}\sum_{x,\,y\in\Phi\cap b(0,\,r)}1_{[0<\|x-y\|\le r]},\ \text{for } r\ge 0. \tag{III.1}$$

where $\boldsymbol{E}_{\mathbf{0}}^{!}$ stands for the expectation with respect to the reduced Palm distribution $P_0^{!}$ of the stationary point process at the origin $(0,0)$. Using the Campbell-Mecke theorem (V.13), we can also write

$$T(r)=\frac{1}{2\lambda^3\ell^d(W)}\boldsymbol{E}\sum_{\substack{x\in\Phi\cap W\\ y,\,z\in\Phi}}1_{[0<\|x-y\|\le r]}1_{[0<\|x-z\|\le r]}1_{[0<\|z-y\|\le r]}\quad , \tag{III.2}$$

when observing the process in any bounded window $W\subset\mathbb{R}^d$ such that $\ell^d(W)>0$. Just like (II.31), this formula serves as the basis for the construction of estimators.

For Φ homogeneous Poisson point process on $\mathbb{R}^2$, the T-function is

$$T(r)=\frac{1}{2}\pi\left(\pi-\frac{3}{4}\sqrt{3}\right)r^4,\ \text{for all } r\ge 0. \tag{III.3}$$

In the special case, that Φ is a homogeneous Poisson point process with distribution P, we know by Silvnyak's theorem (V.16) that for the reduced Palm distribution holds $P_0^{!}=P$. Thus, the T-function becomes

$$T(r)=\frac{1}{2\lambda^2}\boldsymbol{E}\sum_{x,\,y\in\Phi\cap b(0,r)}1_{[0<\|x-y\|\le r]}=\frac{1}{2\lambda^2}\boldsymbol{E}\sum_{x,\,y\in\Phi\cap b(0,r)}^{\neq}1_{[0\le\|x-y\|\le r]},\ \text{for } r\ge 0. \tag{III.4}$$

Using the definition of the factorial moment measure and the fact that the process is stationary we obtain .

$$
\begin{aligned}
2\lambda^2 T(r) &= \int_{b(0,r)} \int_{b(0,r)} 1_{[0\le\|x-y\|\le r]}\, \alpha^2(dx, dy) \\
2\,T(r) &= \int_{b(0,r)} \int_{b(0,r)} 1_{[0\le\|x-y\|\le r]}\, dx\ dy \\
&= \int_{b(0,r)} \ell^2\big(b(0,r)\cap b(x,r)\big)\, dx \\
&= \int_{b(0,r)} 2\ r^2 \arccos\left(\frac{\|x\|}{2\mathrm{r}}\right) - r\ \|x\|\sqrt{1-\frac{\|x\|^2}{4\mathrm{r}^2}}\ dx.
\end{aligned}
$$

Using the polar coordinate system with $x_x = t\ \cos(\theta),\ x_y = t\ \sin(\theta),\ dx = t\ dt\ d\theta,$ we obtain

$$
\begin{aligned}
2\,T(r) &= \int_0^{2\pi} \int_0^r 2\ r^2 \arccos\left(\frac{t}{2\mathrm{r}}\right) - r\ t\ \sqrt{1-\frac{t^2}{4\mathrm{r}^2}}\, t\ dt\ d\theta \\
T(r) &= \pi \int_0^r t\ 2\ r^2 \left(\arccos\left(\frac{t}{2\mathrm{r}}\right) - \frac{t}{2\mathrm{r}}\sqrt{1-\frac{t^2}{4\mathrm{r}^2}}\right) dt.
\end{aligned}
$$

We now provide a second substitution $s = \frac{t}{2\mathrm{r}},\ dt = 2\ r\ ds$

$$
\begin{aligned}
T(r) &= 8\pi\ r^4 \int_0^{\frac{1}{2}} s\ \left(\arccos(s) - s\sqrt{1-s^2}\right) ds \\
&= \frac{1}{2}\pi r^4 \left(\pi - \frac{3}{4}\sqrt{3}\right).
\end{aligned}
$$

We can also compute theoretical result for a Poisson cluster point process Φ. Let P_0 be the Palm distribution at the origin $(0,0)$ of the Poisson cluster process, let P be its original distribution and P_{Cl_0} the Palm distribution of the representative cluster N_C, P_{Cl} being its original distribution. Then

$$
P_0 = P * P_{Cl_0}, \quad \text{where } * \text{ stands for the convolution,} \tag{III.5}
$$

The Palm distribution can be interpreted as the superposition of the Palm distribution at the origin P_{Cl_0} of the cluster and independent point process with the distribution P of the original distribution of Φ.

The Palm distribution P_{Cl_0} of the representative cluster is given for every Y in $\mathcal{N}$ and Borel $B \in \mathcal{B}^d$ by

$$
P_{Cl_0}(Y) = \frac{1}{\varpi} \boldsymbol{E} \sum_{x\in N_c\cap B} 1_{[(N_C\setminus\{x\})\in Y]}, \tag{III.6}
$$

where ϖ is the mean number of daughter points per parent. For every measurable function f it turns into

$$
\int f(\psi)\ P_{Cl_0}(d\,\psi) = \frac{1}{\varpi} \boldsymbol{E} \sum_{x\in N_C\cap B} f(N_C\setminus\{x\}). \tag{III.7}
$$

For a Poisson cluster point process Φ with intensity λ, we have

$$T(r)=T_{Poisson}(r)+\frac{3}{2\lambda\varpi}\boldsymbol{E}\sum_{x,y\in N_c}1_{[0<\|x-y\|\le r]}\ell^{d}\left(b(0,r)\cap b(x-y,r)\right)$$
$$+\frac{1}{2\lambda^{2}\varpi}\boldsymbol{E}\sum_{x,y,z\in N_c}1_{[0<\|x-y\|\le r]}1_{[0<\|x-z\|\le r]}1_{[0<\|z-y\|\le r]}. \tag{III.8}$$

To prove the assertion, we first notice that in such a case, we have three different types of points triplets:

$$\begin{cases}\text{\_case 1: the points in the triplets are in three different clusters (distribution of the process),}\\ \text{\_case 2: two of them can be in one cluster and one point in an other (mixed distribution),}\\ \text{\_case 3: the three of them can be in the same cluster (distribution of the cluster).}\end{cases}$$

Thus, we can write:

$$2\lambda^{2}\,T(r)=\boldsymbol{E}_{\mathbf{0}}^{!}\sum_{x,y\in\Phi\cap b(0,r)}1_{[0<\|x-y\|\le r]}=\underbrace{C_1}_{case\,1}+\underbrace{C_2}_{case\,2}+\underbrace{C_3}_{case\,3}. \tag{III.9}$$

We now provide calculations for these three terms. For C_1:

$$C_1=\int\sum_{x,y\in\varphi\cap\bar{b}(0,r)}1_{[0<\|x-y\|\le r]}P(d\varphi). \tag{III.10}$$

For C_3:

$$C_3=\int\sum_{x,y\in\psi\cap\bar{b}(0,r)}1_{[0<\|x-y\|\le r]}\;P_{Cl_0}(d\psi). \tag{III.11}$$

For C_2:

$$C_2=2\int\int\sum_{x\in\varphi\cap\bar{b}(0,r)}\sum_{y\in\psi\cap\bar{b}(0,r)}1_{[0<\|x-y\|\le r]}\;P(d\varphi)\;P_{Cl_0}(d\psi). \tag{III.12}$$

For the first term C_1 we use the Campbell-Mecke theorem (V.13-V.14) for positive measurable function and the definition of P_0 (III.5).

$$\begin{aligned}C_1&=\lambda\int\int\sum_{y\in\varphi\cap b(0,r)}1_{[0<\|x-y\|\le r]}\;P_0^{!}(d\varphi)\;dx\\&=\lambda\int\int\sum_{y\in\varphi\cap\bar{b}(0,r)}1_{[0<\|x-y\|\le r]}\;P_0(d\varphi)\;dx\\&=\lambda^{2}\int_{b(0,r)}\int_{b(0,r)}1_{[0<\|x-y\|\le r]}\;dx\;dy+\lambda\int_{b(0,r)}\sum_{y\in\varphi\cap\bar{b}(0,r)}1_{[0<\|x-y\|\le r]}\;P_{Cl_0}(d\varphi)\;dx.\end{aligned} \tag{III.13}$$

For the second term C_2 we make use of the stationarity of the process.

$$
\begin{aligned}
C_2 &= 2\int \sum_{y\in\psi\cap\bar{b}(0,r)} \left(\int \sum_{x\in\varphi\cap\bar{b}(0,r)} 1_{[0<\|x-y\|\le r]}\, P(d\varphi) \right) P_{Cl_0}(d\psi) \\
&= 2\lambda \int \sum_{y\in\psi\cap\bar{b}(0,r)} \left(\int 1_{[0<\|x-y\|\le r]} 1_{[x\in\bar{b}(0,r)]}\, dx \right) P_{Cl_0}(d\psi) \\
&= 2\lambda \int \sum_{y\in\psi\cap\bar{b}(0,r)} \ell^d\left(b(0,r)\cap b(y,r)\right) P_{Cl_0}(d\psi).
\end{aligned}
\qquad \text{(III.14)}
$$

Combining the previous results (III.13) and (III.14) with the formula (III.7) leads to the result.

We can now calculate the function for Gauss-Poisson processes. For a Gauss-Poisson process Φ on $\mathbb{R}^2$ with q_1 and q_2 standing for the probabilities that there will be one and two offsprings respectively and s being the distance between offsprings in the same cluster, the T-function is

$$
T(r) = T_{Poisson}(r) + \frac{3q_2}{\lambda(q_1+2q_2)} 1_{[s\le r]}\, 2\, r^2 \left(\arccos\left(\frac{s}{2r}\right) - \frac{s}{2r}\sqrt{1-\frac{s^2}{4r^2}} \right). \qquad \text{(III.15)}
$$

For such a point process, we can't find triplets belonging to the same cluster, these last having a maximum of two points. In the case we have two points in the same cluster, the distribution of the second, knowing the first is some x, is the uniform distribution on the perimetre of $b(x,s)$ and that leads us to the result.

Remark 1: It seems impossible to calculate explicit theoretical results for the T-function for other point processes.

Remark 2: In addition to the first statement, it is impossible to calculate theoretical results for the variability of the T-function.

2. Estimators for the T-function

In order to investigate the behaviour of the function by means of simulation, we will now work on calculating estimators we will use for this purpose. There will be three of them, distinguished by the edge-correction used: the border one, the translation correction one and the isotropic correction one. Basis for the construction of these estimators is the second definition (III.2) we gave for the T-function and that we now recall:

$$
T(r) = \frac{1}{2\lambda^2\, \ell^2(B)} \boldsymbol{E} \sum_{\substack{x\in\Phi\cap B \\ y,z\in\Phi}} 1_{[0<\|x-y\|\le r]} 1_{[0<\|x-z\|\le r]} 1_{[0<\|z-y\|\le r]}\ , \qquad \text{(III.16)}
$$

for every Borel $B\in\mathcal{B}_0^2$. B has to have strictly positive volume for the expression on the left side to be well defined.

a) Border method

As we may not see in the window we use for observation every triplets - points being too close to the border may have unseen neighbours - we consider only those triplets in which one point at least is further away than r from the border of the window W. We immediately infer from above the following estimator for $\lambda^2 T(r)$

$$\widehat{\lambda^2 T(r)}_b = \frac{1}{2\Phi(W_{-b(0,r)})} \sum_{\substack{x \in \Phi \cap W_{-b(0,r)} \\ y,z \in \Phi}} 1_{[0<\|x-y\|\le r]} 1_{[0<\|x-z\|\le r]} 1_{[0<\|z-y\|\le r]} \quad , \qquad \text{(III.17)}$$

where $W_{-b(0,r)}$ is the eroded window $W \setminus \{x \in W : \inf_{y \in \partial W} \|x-y\| \le r\}$. This is defined for every r such that $\Phi(W_{-b(0,r)}) > 0$. This estimator is ratio unbiased.

b) Translation correction method

In this case we use every point we see in the bounded window W and for each triplet we use a weight function that describes the probability that the triplet is observed. The estimator is now defined as follows

$$\widehat{\lambda^3 T(r)} = \frac{1}{2\ell^2(W)} \sum_{x,y,z \in \Phi} 1_{[0<\|x-y\|\le r]} 1_{[0<\|x-z\|\le r]} 1_{[0<\|z-y\|\le r]} k(x,y,z) \quad , \qquad \text{(III.18)}$$

where k is the weight function, chosen so that the estimator would be unbiased. The usual choice is that $\frac{1}{k}$ is the measure of all transformations under which the triplet remains in the window. We will use the one chosen by Schadlitz K. and Baddeley A.J. in [12], that is

$$k_t(x,y,z) = \frac{\ell^2(W)}{\ell^2(W_x \cap W_y \cap W_z)} \quad , \qquad \text{(III.19)}$$

where W_x (respectively W_y, W_z) denotes the translation of the original window W by x (respectively by y and z). Further details can be found in [12]. In this case, we get the following estimator

$$\widehat{\lambda^3 T(r)}_t = \frac{1}{2} \sum_{x,y,z \in \Phi \cap W} 1_{[0<\|x-y\|\le r]} 1_{[0<\|x-z\|\le r]} 1_{[0<\|z-y\|\le r]} \frac{1_{[\ell^2(W_x \cap W_y \cap W_z) \ne 0]}}{\ell^2\left(W_x \cap W_y \cap W_z\right)} \quad . \qquad \text{(III.20)}$$

The definition is correct and the estimator unbiased as long as $\ell^2(W_x \cap W_y \cap W_z) > 0$. As we already saw in Chapter II, this is always true if we observe the process in a square window with side longer than r.

c) Isotropic correction method

This will be the last method we use. We now choose the weight funcion k so that the ratio $\frac{1}{k}$ is the angular measure of all rotations around x under which y and z remain in the window W.

It is an analogy to Ripley's isotropic correction for the K-function. The centre of rotation is always the point x and the angle of rotation the angle $\widehat{yxz}$ anticlockwise (that means the angle is the same if we consider the triplet (x,y,z) or if we consider (x,z,y)).

We first consider the angles that leave $\partial b(x,y)$ inside our window W. Then, we rotate the window anticlockwise according to the angle $\widehat{yxz}$ and consider angles that leave $\partial b(x,z)$ in the rotated window W_{rot} (the centre of the rotation is x). We obtain our weight k_{ic} by summing on the angles that leave both $\partial b(x,y)$ and $\partial b(x,z)$ respectively in W an W_{rot}.

If we consider the triplet (x,y,z) and denote $\tau=\widehat{yxz}$ the angle of the rotation around x and $\vec{e}_\beta$ the unit vector forming the angle β with the horizontal axis, then the formula giving k_{ic} is

$$\frac{1}{k_{ic}(x,y,z)}=\frac{1}{2\pi}\int_0^{2\pi} 1_{[x+\|x-y\|\,\vec{e}_\beta]}\,1_{[x+\|x-z\|\,\vec{e}_{\beta+\tau}]}\,d\beta. \tag{III.21}$$

Once again, further details are to be found in [12]. Finally, the estimator is of the form

$$\widehat{\lambda^3 T(r)}_i=\frac{1}{2\ell^2(W)}\sum_{x,y,\,z\in\Phi\cap W} 1_{[0<\|x-y\|\le r]}\,1_{[0<\|x-z\|\le r]}\,1_{[0<\|z-y\|\le r]}\,\frac{2\pi\;1_{[k_{ic}(x,y,z)\neq 0]}}{k_{ic}(x,y,z)}. \tag{III.22}$$

The estimator is unbiased for all r such that $\partial b(x,r)\cap W\neq\emptyset$ for any $x\in\Phi\cap W$. For a squared window, this is true for r smaller than half of the length of the diagonal.

To get the three estimators $\widehat{T(r)}_b$, $\widehat{T(r)}_t$ and $\widehat{T(r)}_i$ for the $T-$function, we respectively divide (III.17) by $\frac{\Phi(W)^2-\Phi(W)}{\ell^2(W)}$ and (III.20) and (III.22) by $\frac{\Phi(W)(\Phi(W)-1)(\Phi(W)-2)}{\ell^2(W)}$. These estimators are ratio-unbiased.

3. Definition and properties of the z-function

We now introduce the z-function, an other third order characteristic which was defined by Møller J. et al. in [5]. For any stationary simple point process Φ with finite and strictly positive intensity ρ, strictly positive pair correlation function $g(s_1,s_2)=g(s_1-s_2)$ and density of the third order moment measure $\rho^{(3)}(s_1,s_2,s_3)=\rho^{(3)}(s_2-s_1,s_3-s_1)$ we define z as

$$z(r)=\frac{1}{\pi^2 r^4}\int_{\|t\|\le r}\int_{\|u\|\le r}\frac{\rho^{(3)}(t,u)}{\rho^3 g(t)g(u)g(t-u)}\,du\,dt,\ \text{for } r>0. \tag{III.23}$$

That is, using a similar definition as for the T-function (II.1),

$$z(r)=\frac{1}{\pi^2 r^4 \rho^2}\boldsymbol{E}_{\mathbf{0}}^{!}\sum_{t,u\in\Phi,\|t\|\le r,\|u\|\le r}^{\neq}\frac{1}{g(t)g(u)g(t-u)},\ \text{for } r>0. \tag{III.24}$$

where $\boldsymbol{E}_{\mathbf{0}}^{!}$ denotes expectation with respect to the reduced Palm distribution $P_0^!$ at the origin. One can see that definitions are similar and only differ by the use of the pair correlation of the process as a weight function and the fact that there is no more condition on the inter-point distance between the second and the third point.

For the log-Gaussian Cox process defined in Chapter II, the formula simplifies to become

$$z(r)=1, \quad r>0. \tag{III.25}$$

This result is obtained by use of (II.37) and (II.38).

For a Poisson point process, the z-function also has a simple expression. We know from Chapter II that the pair correlation function of a Poisson process is equal to 1. Thus, the expression (III.24) simplifies and the function is given by

$$\begin{aligned} z(r) &= \frac{1}{\pi^2 r^4 \rho^2} \boldsymbol{E}_{\mathbf{0}}^{!} \sum_{t,u\in\Phi,\|t\|\le r,\|u\|\le r}^{\neq} 1 \\ &= \frac{1}{\pi^2 r^4 \rho^2} \boldsymbol{E}_{\mathbf{0}}^{!} \sum_{t,u\in\Phi\cap b(0,r)}^{\neq} 1 \quad . \end{aligned} \tag{III.26}$$

4. Estimators for the z-function

a) Border method

Just like for T, we give a first and simple estimator based on the border method. If we observe the process in a bounded window $W\in\mathbb{R}^2$, one point has to lie in the eroded window $W_{-b(0,r)}$. Following what we did for (III.17), we get the following unbiased estimator

$$\widehat{\ell^2(W_{-b(0,r)})z_b(r)} = \frac{1}{\pi^2 r^4 \rho^3} \sum_{\substack{x\in\Phi\cap W_{-b(0,r)},\ y,z\in\Phi \\ \|x-y\|\le r,\ \|x-z\|\le r}}^{\neq} \frac{1}{g(x-y)g(x-z)g(y-z)} \quad . \tag{III.27}$$

b) Isotropic correction method

Further we can define an other, better, estimator for the z-function for a stationary and isotropic simple point process on the plane $\mathbb{R}^2$ observed in a bounded window W. The estimator is again based on the one introduced by Ripley for the K-function and the weight function is exactly the same as the one we introduced for the T-function in the isotropic correction method (III.21). The only difference is that in the case we are now interested in, we use in addition the pair correlation function of the process. Thus, we will use the same notations.

For any point process Φ that has the above properties, we define the following estimator

$$\widehat{\ell^2(W)r^4\rho^3 z_i(r)} = \frac{2}{\pi^2} \sum_{\substack{x\in\Phi,\ y,z\in\Phi\cap W\setminus\{x\} \\ \|x-y\|\le r,\ \|x-z\|\le r}}^{\neq} \frac{2\pi 1_{[k_{ic}(x,y,z)]}}{k_{ic}(x,y,z)\,g(\|x-y\|)g(\|x-z\|)g(\|y-z\|)} \tag{III.28}$$

This is an unbiased estimator for any r that satisfies the following condition

$$r \;<\; \boldsymbol{inf}\left\{ r>0 : \int_{x_1\in W}\int_{a\in(0,r)}\int_{b\in(0,r)}\int_{\theta\in(0,2\pi)} 1_{[\frac{2\pi k_{ic}}{k_{ic}}=\infty]}\, d\theta\, da\, db\, dx_1 \;>\; 0 \right\}. \tag{III.29}$$

To prove that it is unbiased, we use the Campbell's theorem and the formula (III.21). For a point process Φ and every strictly positive measurable function h we have

$$\boldsymbol{E} \sum_{x_1,\dots,x_n \in \Phi}^{\neq} h(x_1,\dots,x_n) = \int \dots \int h(x_1,\dots,x_n)\, \alpha^{(n)}(dx_1,\dots,dx_2)$$

$$= \int \dots \int h(x_1,\dots,x_n)\, \rho^{(n)}(x_1,\dots,x_n)(dx_1,\dots,dx_2),$$

where $\alpha^{(n)}$ is the n-th factorial moment measure. Thus, the mean of our estimator will be

$$\boldsymbol{E} \sum_{\substack{x \in \Phi \cap W,\ y,z \in \Phi \cap W \setminus \{x\} \\ \|x-y\| \le r,\ \|x-z\| \le r}}^{\neq} \frac{2\pi\, 1_{[k_{ic}(x,y,z)]}}{k_{ic}(x,y,z)\, g(\|x-y\|)\, g(\|x-z\|)\, g(\|y-z\|)}$$

$$= \int_W \int_W \int_W K \frac{\rho^{(3)}(x,y,z)}{g(\|x-y\|)\, g(\|x-z\|)\, g(\|y-z\|)} 1_{[0<\|x-y\|\le r]} 1_{[0<\|x-z\|\le r]} 1_{[0<\|y-z\|\le r]}\, dx\ dy\ dz$$

$$= \int_W \int_W \int_W K \frac{\rho^{(3)}(a,b,\tau)}{g(a)\, g(b)\, g(f(a,b,\tau))} 1_{[0<a\le r]} 1_{[0<b\le r]}\, dx\ dy\ dz$$

$$= \int_W \int_{(0,r)} \int_{(0,r)} \int_{(0,2\pi)} \int_{(0,2\pi)} \frac{\rho^{(3)}(a,b,\tau)}{g(a)\, g(b)\, g(f(a,b,\tau))}\ 1_{[x+a\,\vec{e}_\beta]}\ 1_{[x+b\,\vec{e}_{\beta+\tau}]}\ ab\ d\beta\ d\tau\ da\ db\ dx$$

$$= \ell^2(W) \int_{(0,r)} \int_{(0,r)} \frac{\rho^{(3)}(a,b)}{g(a)\, g(b)\, g(a-b)}\ da\ db,$$

where we provided the substitutions $a = \|x-y\|$, $b = \|x-z\|$. The condition on r gives the third equality.

Like for T, we don't have an estimator for z but an unbiased estimator for $\ell^2(W) r^4 \rho^3 z(r)$. Thus, we divide the results by

$$\ell^2(W) \pi^2 r^4 \widehat{\rho^3},$$

where we choose $\widehat{\rho^3} = \dfrac{\Phi(W)\cdot(\Phi(W)-1)\cdot(\Phi(W)-2)}{(\ell^2(W))^3}$ which is unbiased for the Poisson process. As we provided simulations in a unit square window, it simplifies in $\pi^2 r^4 \widehat{\rho^3}$.

Chapter IV

Simulations

Through simulations, our aim was to test the behaviour of T and z for various point processes. We also wanted to compare the estimators we introduced and see if one would eventually perform better than the others. At last, and even though the functions were not thought for the same processes, we wanted to know which one of them would best discriminate between two processes.

For our studies, we first generated two hundred processes of various kinds (listed below). For simplification, we retained a model in a square window with volume one. In this purpose we used the software R, which already contains source code for a large number of processes. In order to get reliable comparisons, we always considered processes with similar intensity, that is intensity around 400 per unit area (here $1*1$). For each model in our study, we computed the results for all generated processes with a program in C (source code on the cd).

List of the processes used in the study:

Homogeneous Poisson
Baddeley-Silverman
Gauss-Poisson
Thomas
Matérn cluster
Matérn type I
Log-Gaussian Cox

When available, the theoretical value of the function was drawn in blue. That is, for the T-function, for Poisson and Gauss-Poisson processes and for the z-function, for the log-Gaussian Cox process.

For the T-function,

- $\widehat{T}_b$ in brown;
- $\widehat{T}_t$ in red;
- $\widehat{T}_i$ in green.

We chose the stationary Poisson point process with intensity 400 has the reference process for the T-function and first conducted simulations for this process. We already have for it theoretical values for both the function T and its transformed (see III.3).

The function itself is not very useful if we do not use a transformation of some kind. It is clear from *Fig. VI.1* that it is difficult to distinguish between the three estimators and the theoretical value of T. In order to see clearly the differences, we apply the following transformation

$$\sqrt[4]{\frac{2\widehat{T(r)}}{\pi(\pi-\frac{3}{4}\sqrt{3})}} - r \quad . \tag{VI.1}$$

Combining (VI.1) with definition (III.3) of the T-function for a Poisson point process, we obtain that the transformed theoretical value is equal to 0.

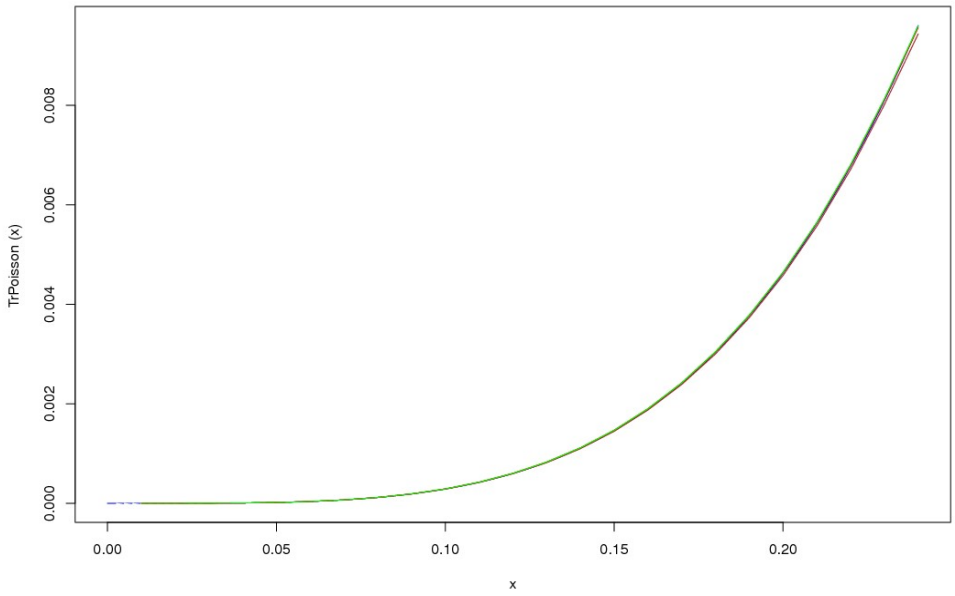

Fig. IV.1: plot of the T-function for a stationary Poisson process with intensity 400.

In this example, we see from *Fig. IV.2* that the translation correction estimator $\widehat{T}_t$ performs slightly better than the isotropic correction one $\widehat{T}_i$, but do not differ much and are almost equal for $r \leq 0{,}12$. On the other hand, the estimator $\widehat{T}_b$ using the border method is, as expected, strongly biased and quickly drops down for greater values.

As the T-function was thought in an attempt to distinguish between the Poisson point process and the cell process introduced by Baddeley A.J. and Silverman B. [3], the last having the same first and second order characteristics as the first (the cell process is a counterexample to the claim that the K-function completely characterises a point pattern), we also provided simulations for the cell process.

Let us first remind how the process is built (definition from [14]): A cell process is generated by dividing space into equal rectangular tiles. In each tile, a random number N of points is placed, where N takes the values *0*, *1* and *10* with probabilities *1/10*, *8/9* and *1/90* respectively. The points within a tile are independent and uniformly distributed in that tile, and the numbers of points in different tiles are independent random integers. In this study, we chose a square unit window divided in $20 \times 20 = 400$ tiles. Thus, for each generated process, the theoretical intenisty is 400 and there should be around 4 to 5 clusters containing 10 points. T being sensitive to clustering, it

should detect it for small values of r and be somehow similar to what we got for the Poisson process for greater values.

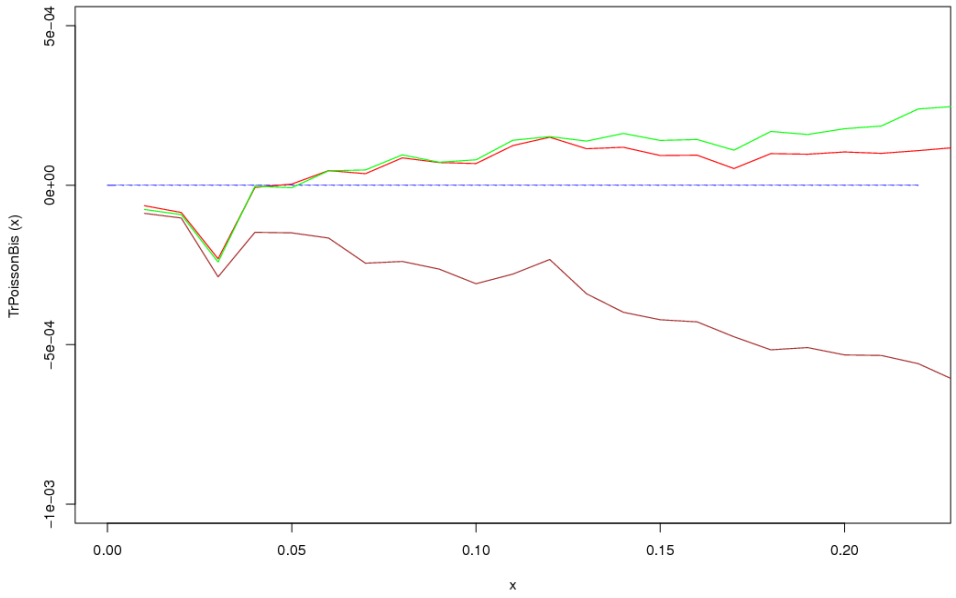

Fig. IV.2: transformed values of the estimators (according to (IV.2)) for the same stationary Poisson point process as in Fig. IV.1.

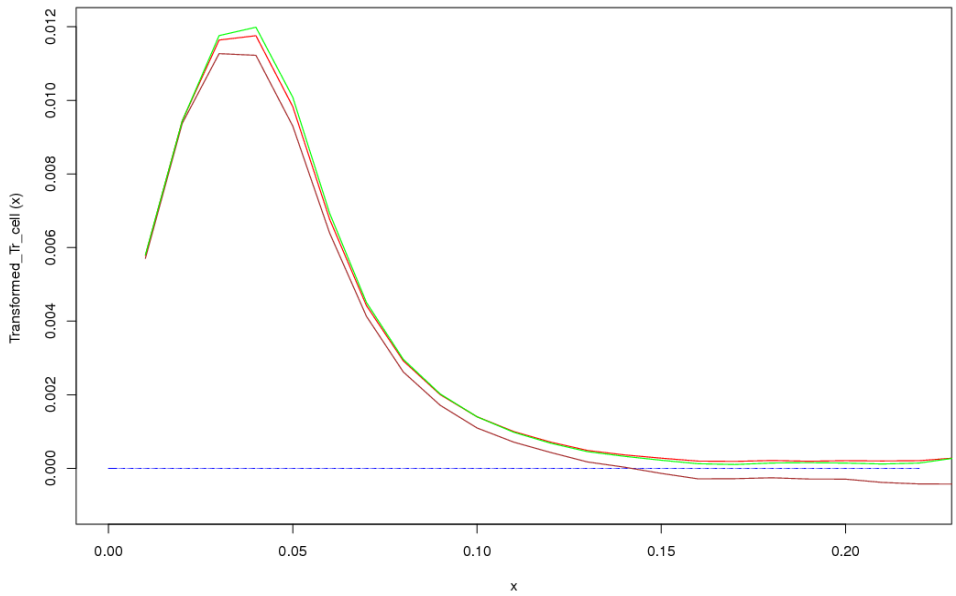

Fig. IV.3: transformed values of the estimators for a cell process with 400 hundred square tiles.

Simulations proceeded as expected. The T-function is clearly more sensitive to clustering than the K-function and proves successful to discriminate between the two processes whereas K was not.

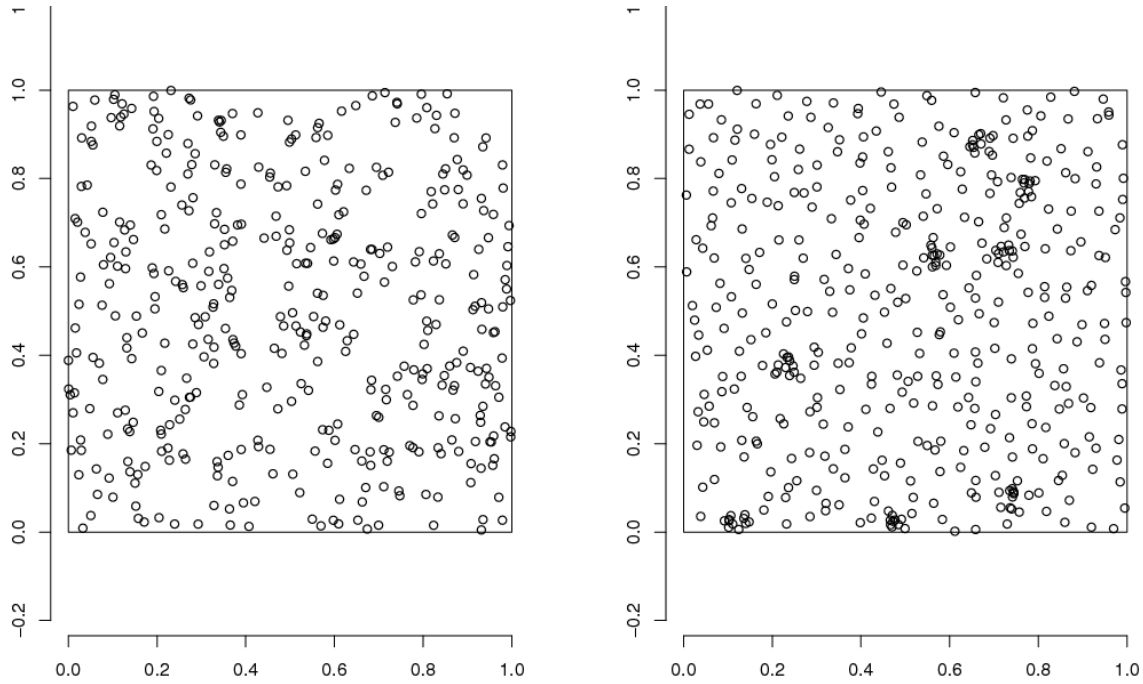

Fig. IV.4: Left: realization of a stationary Poisson point process with intensity 400 hundred. Right: Baddeley and Silverman's process with 400 hundred tiles; seven clusters can be seen in the window.

We conducted simulations for other clustered processes. For Thomas process, Matérn's Cluster process and Gauss-Poisson process. For all of them, we generated realizations with various parameters. The aim is first to compare results with the ones obtained previously for the cell process; then to see how the parameters affect the function itself.

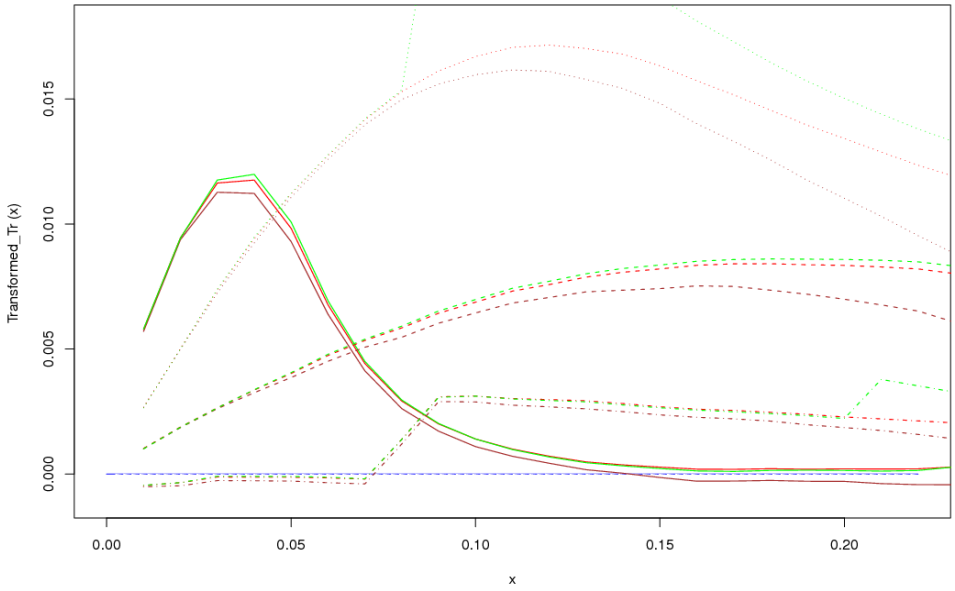

Fig. IV.5: transformed values of the estimators for Baddeley ans Silverman's cell process with 400 tiles (lines); Matérn cluster process with cluster intensity 4 and cluster radii 0,08 (dots); Thomas process with cluster intensity 4 and variance 0,08 (dashes); Gauss-Poisson process with intensity of the parent process 266, probability for a cluster of having two points 0,5 and diameter of the clusters containing two points 0,8 (dots and dashes). Both Matérn and Thomas process have intensity of the parent process equal to 100.

As we can see from the realizations in *Fig. IV.4* and *Fig. IV.6*, Matérn cluster process has a slightly smaller mean interaction distance between points belonging to a same cluster than has the Thomas process. Thus, it looks a bit more concentrated in some areas of the window than the Thomas process. These differences can also be seen in *Fig. IV.5* where the T-function takes higher absolute values for the Matérn cluster process than for the Thomas one, the peak being also reached earlier. The clusters for these two processes are different from the ones in the cell process; this last has fewer clusters,denser (10 points and a maximum inter-point distance equal to $\sqrt{2}\times 0{,}05$ for the cell process; 8 points and a maximum inter-point distance equal to 0,08 for the Matérn cluster process) and T reaches a peak at first for this process. At last, and as one could expect from the definition of the Gauss-Poisson process, T takes the same values as in the Poisson case for r smaller than the diametre of the clusters containing exactly two points: for this value we can see a small jump. Each cluster consisting in only two points, there is no dense clustering for this kind of process.

When we modify the intensity of the parent process, but keep the same intensity for the process,we also have to change the cluster intensity. The T-function can discriminate between two such processes, the process having the fewest parents but the most points in cluster taking higher values than the other process, as shown in *Fig. IV.7*.

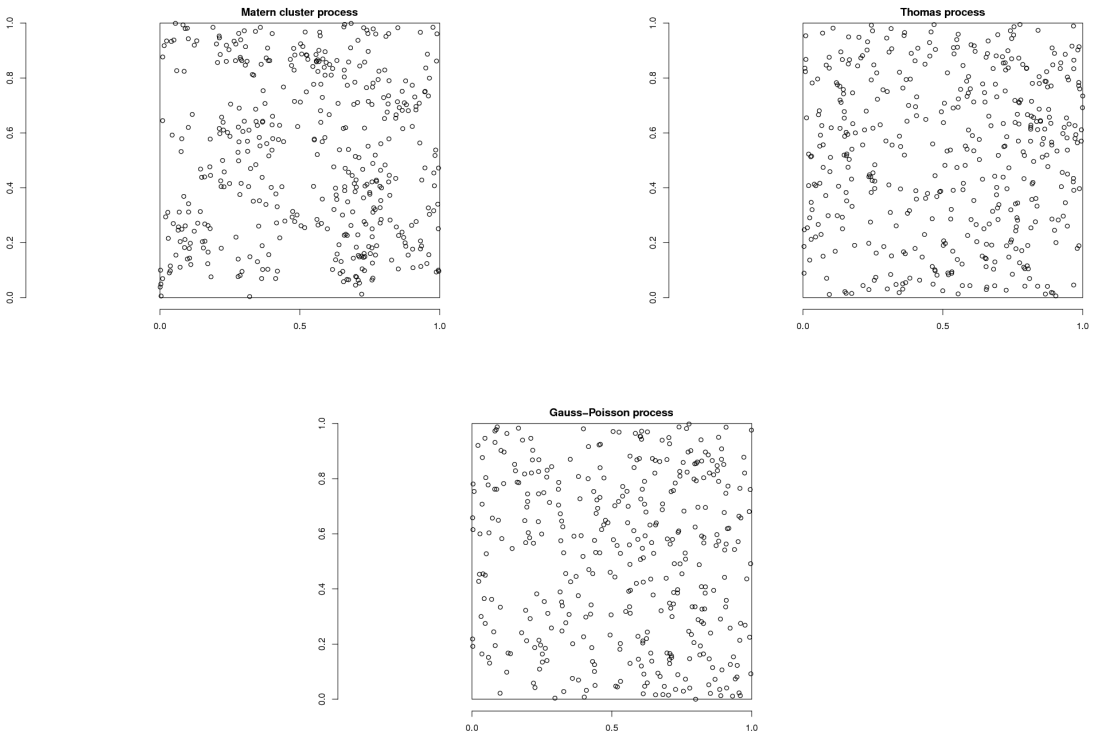

Fig. IV.6: realizations of a Matérn cluster process with parameters 100-0,08-4; of a Thomas process with parameters 100-0,08-4; of a Gauss-Poisson process with parameters 266-0,08-4.

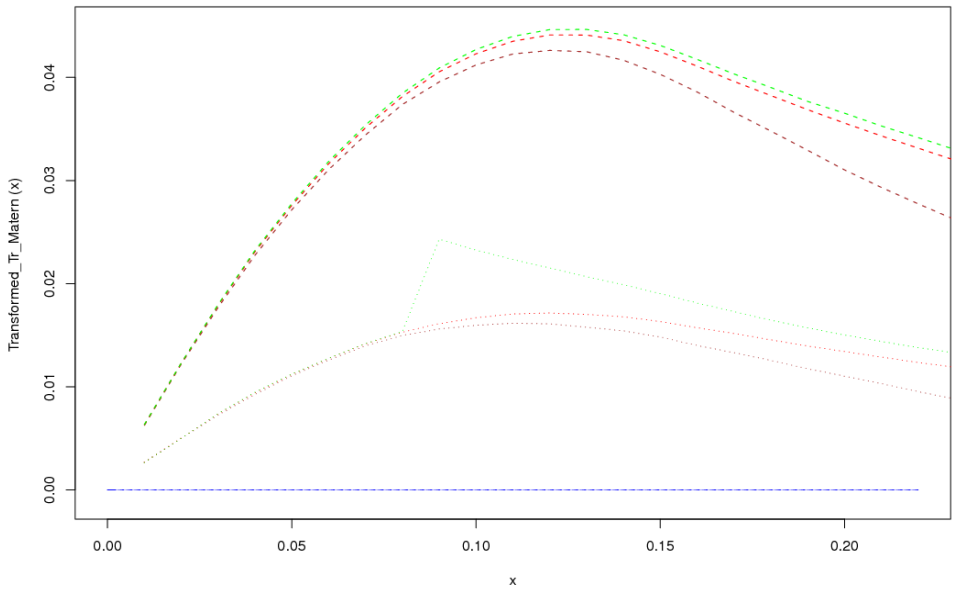

Fig. IV.7: transformed values of the estimators for the Matérn cluster process for various parameters: intensity of the parent process 100 and cluster intensity 4 (dots), intensity of the parent process 33 and cluster intensity 13 (dashes). The radius is the same and equal to 0,08.

To complete our study of T for Matérn cluster processes, we include a graph showing the results for various values of the radii of the clusters, but same intensities for the parent process and the clusters.

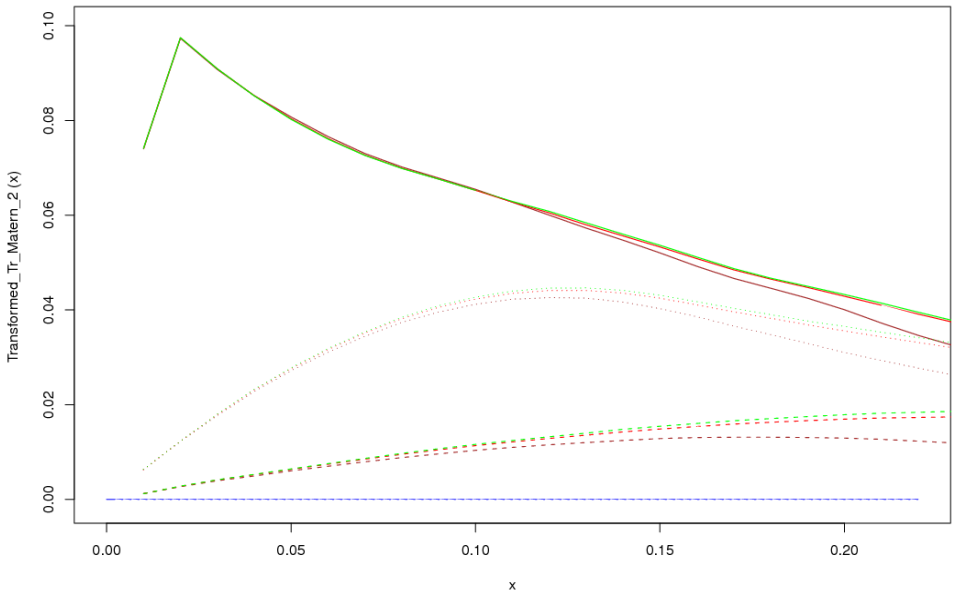

Fig. IV.8: transformed values for the Matérn cluster process for various radii of the clusters: 0,01 (lines); 0,08 (dots); 0,2 (dashes). The intensity of the process is the same and equal to 399 (33×13).

In this situation, we see that the smaller the radius is, the sooner we observe the peak and the higher the values are. For great values of the radius, the curve appears to be almost flat, and then tending to the stationary Poisson. When the radius of the clusters increases such, that the ratio with the size of the window is almost one, we can see the process as a superposition of stationary Poisson processes and then a stationary Poisson process itself. Typical realizations of the Matérn cluster processes used in the study can be seen in *Fig. IV.9*.

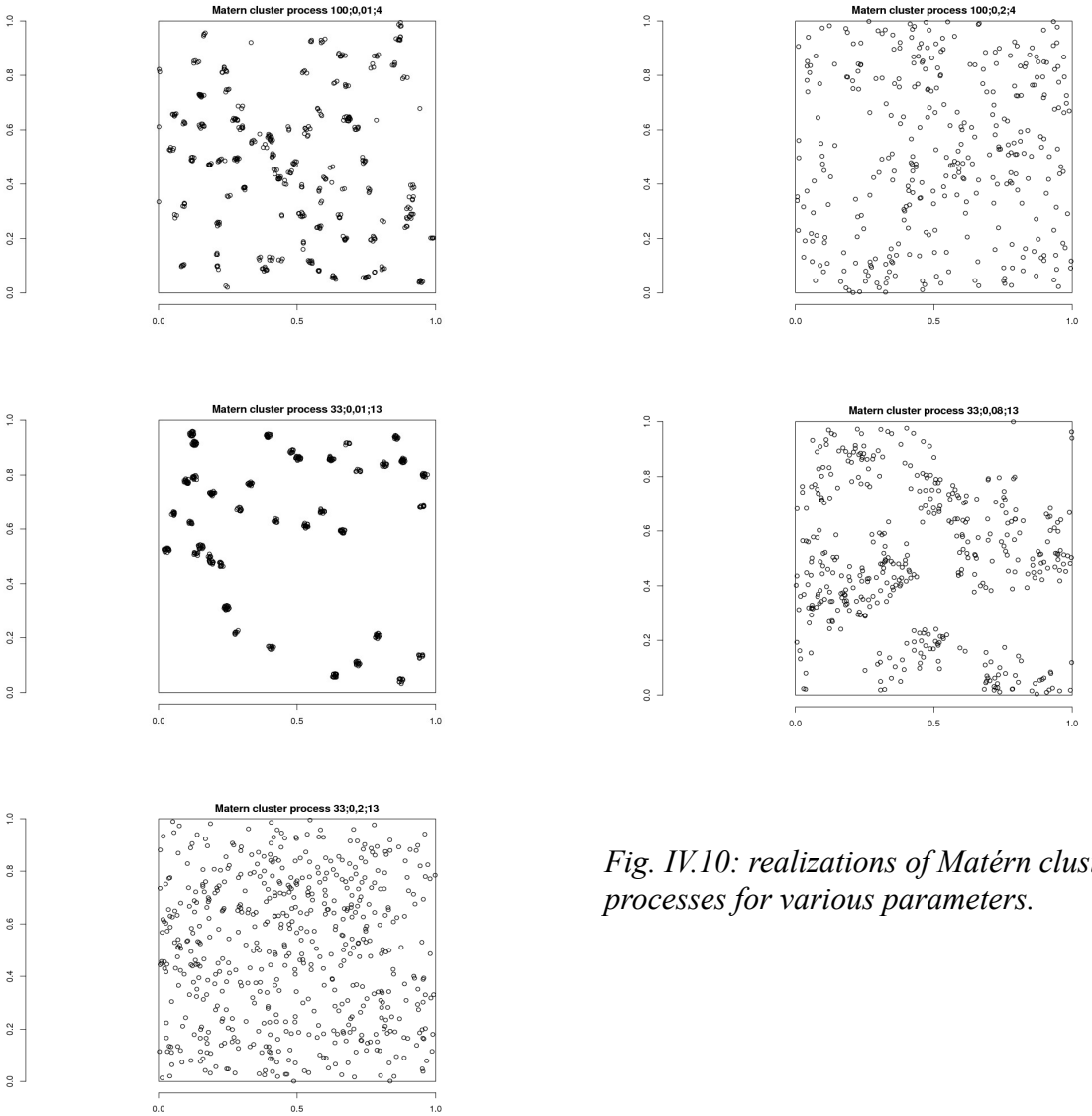

Fig. IV.10: realizations of Matérn cluster processes for various parameters.

We conducted the same simulations for a last kind of clustering process, the Gauss-Poisson process. Like for the stationary Poisson process, theoretical results are known (see (III.15)).

We simulated realizations for various parameters of the intensity λ of the Poisson parent process and adapted the probability p of having two parents in a cluster so that the intensity λ_{GP} of the process would be almost 400: we chose respectively $\lambda = 320\,;266\,;220$ and $p = 0{,}2\,;0{,}5\,;0{,}8$. That is respectively $\lambda_{GP} = 384\,;399{,}5\,;396$. Each time we did it for inter-point distance in a same cluster equal to $0{,}01$ and $0{,}08$. We gave here the results for $\lambda = 320$ (see *Fig. IV.10*).

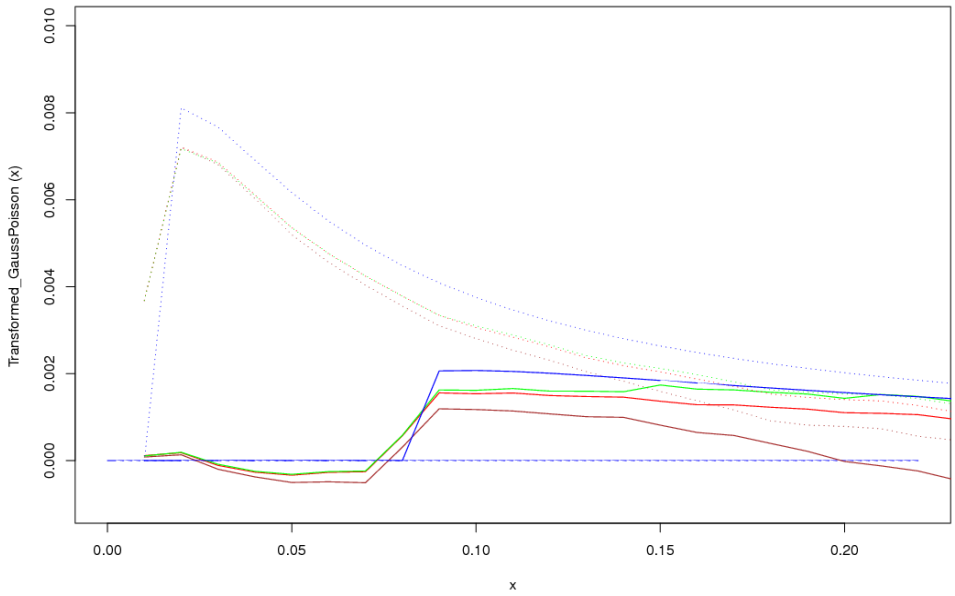

Fig. IV.10: realizations of Gaus-Poisson processes with intensity of the Poisson process equal to 320 and probability of having two points in a cluster 0,2. The radius of the cluster is respectively 0,01 (dashes) and 0,08 (lines). Theoretical values are in blue.

Results are as expected and do not differ much of the theoretical value. The jump for values greater than the radius of the clusters can be clearly observed. For these parameters, it appears that the isotropic correction is slightly better than the translation one; that was not the case for the Poisson process.

We provided the same study for a regular process, that underwent thinning, the MatérnI hard-core process. We will again study how T behaves for such processes and how a change in parameters affects it.

As we compare the process with a stationary Poisson point process with intensity 400, we chose 600 as the intensity of the Poisson process and 0,015 as the inhibition distance for the MaternI process. This gives, according to (II.58) a total intensity almost equal to 400 (precisely 392,609). Nonetheless, a stationary Poisson process describes complete randomness: that implies that some points may lie close to each other, whereas in a regular process, this is not possible due to the inhibition distance. There should be a greater number of triplets for small values of r in the case of the Poisson process and a difference in the aspect of the curve should be noticed for such values.

As we can observe on *Fig. IV.11*, results fulfill expectations. Here, the T-function clearly distinguish the two kinds of processes and the drop observed indicates that there is no triplet for small values of r in the regular case. Then, the greater r is, the closer it is from T in the Poisson case. For the greatest values, it does not differ significantly, as we could suppose from the definition of the process.

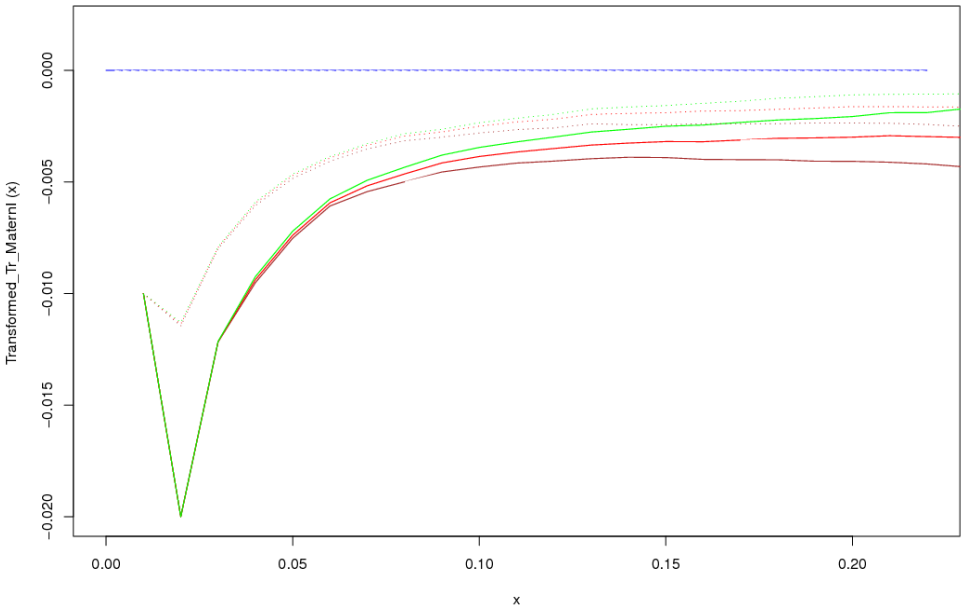

Fig. IV.11: transformed values of the estimators for MatérnI process with intensity of the Poisson process 600 and inhibition distance 0,02 (lines) and 0,015 (dashes).

We also observed how the function reacts when changing the intensity of the parent process but keeping the same inhibition distance.

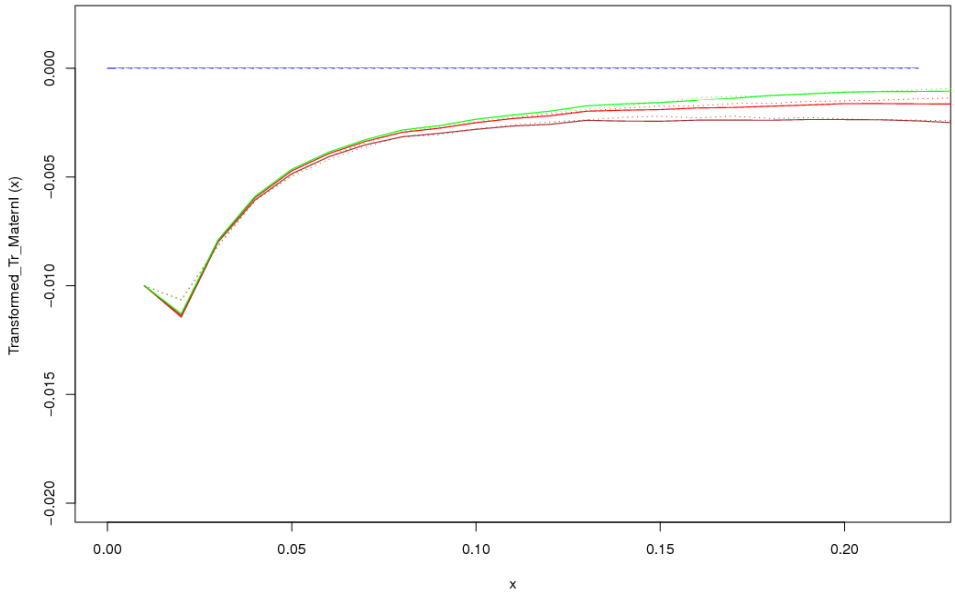

Fig. IV.12: the same for various intensities of the parent processes: 600 (lines) and 400 (dots). The inhibition distance is the same and is equal to 0,015.

In such a case,the transformed T gives the same results for the two processes, the estimated values are the same even though the intensities differ. This is no surprise, as we divide by an unbiased estimator of the intensity. Realizations of the processes can be seen in *Fig. IV.13* below.

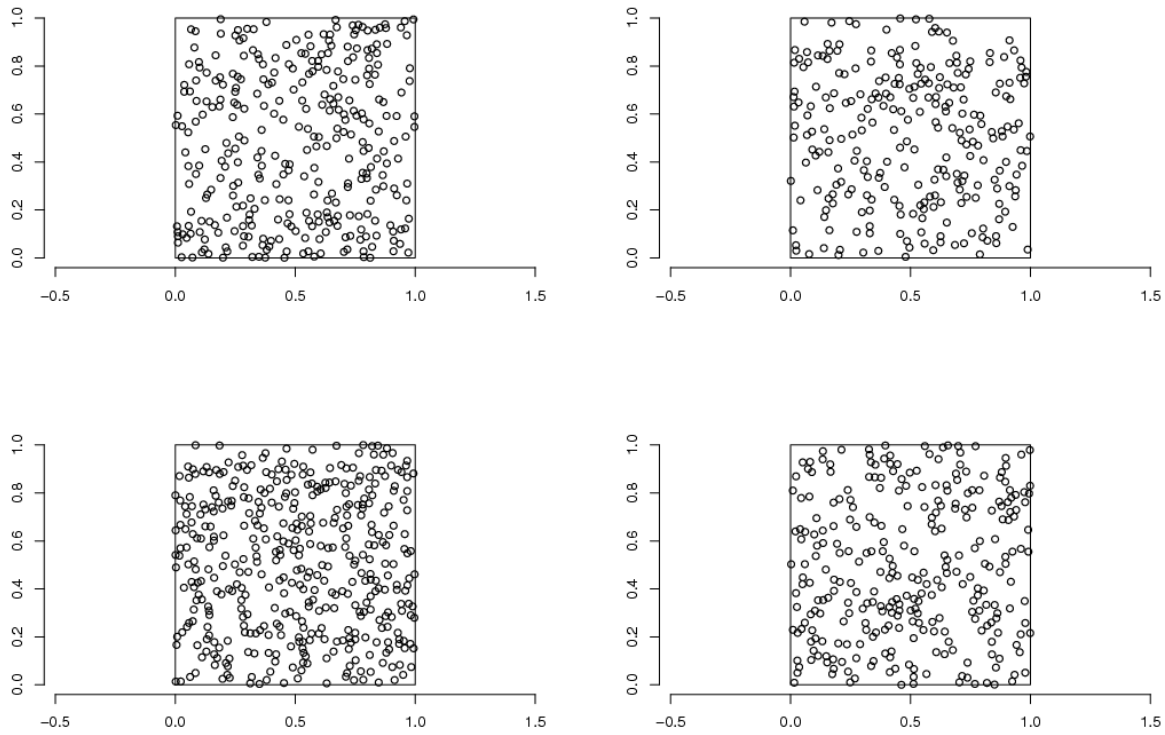

Fig. IV.13: MatérnI hard-core processes. Top left: intensity of the Poisson process 400, inhibition distance 0,015. Top right: intensity of the Poisson process 400, inhibition distance 0,02. Bottom left: intensity of the Poisson process 600, inhibition distance 0,015. Bottom right: intensity of the Poisson process 600, inhibition distance 0,02.

To conclude the study of T we calculated the variance for the three estimators; our goal is to know how much variation there is from the mean. To do so we used the standard approximation $S^2=\frac{1}{n-1}\sum_{i=1}^{n}(X_i-\bar{X})^2$ (see [1]) which is unbiased.

For the cases we studied, it appears that the variability is smaller for the isotropic correction. As one could infer from its definition, the border method is the worse, the lack of information for great values of r playing an important role. The results for the Poisson, the Gauss-Poisson and the MatérnI process are shown in *Fig. IV.14*.

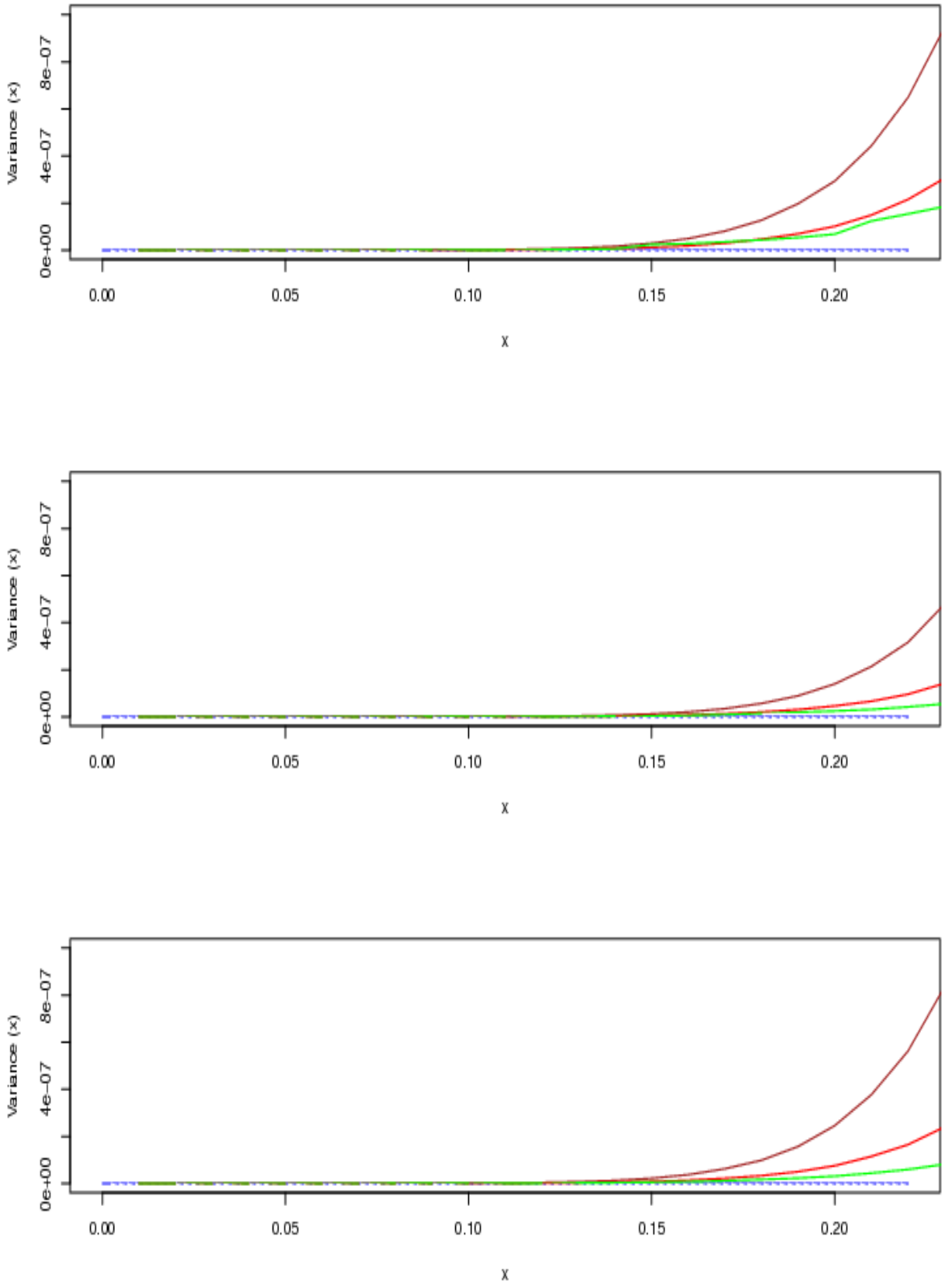

Fig. IV.14: variance of the estimators for the border method (brown), the translation method (red), the isotropic method (green). Top: Gauss-Poisson process (320-0,08-0,2). Middle: Matérn hard-core type I (600-0,015). Bottom: Poisson (400).

We provided simulations for the z-function following the same basis. We did the study only for four kind of processes, for which we were able calculate the pair-correlation function. These are: the Poisson process, the Matérn Cluster process, the Thomas process and the log-Gaussian process.
The z-funtcion is similar to T up to the fact that we use an expression involving the pair-correlation function and that there is no more condition on the distance between the points y and z, whereas previously the points had to lie within $b(x,r)$ and also be at a maximum distance r. This has a direct influence on the calculus, this one being much longer. In addition, the function does not give stable results for small values of r (see [5], fig. 9.). Thus we calculated z for values up to 0,4 but restricted ourselves to the border correction.

For the Poisson process, the pair-correlation function is equal to 1 (see (II.20) and (II.38)). Thus, the estimators $\widehat{\pi^2 r^4 \lambda^3 z(r)}$ are simple. We also recall the form of the pair-correlation function for the other processes. For the Matérn cluster process, the pair-correlation function is of the form (see (II.54))

$$g(\|x-y\|)=\begin{cases} 1+\dfrac{2}{\lambda_{P_1}\pi^2 r^2}\cdot\left(\arccos\left(\dfrac{\|x-y\|}{2\mathrm{r}}\right)-\dfrac{\|x-y\|}{2\mathrm{r}}\sqrt{1-\left(\dfrac{\|x-y\|}{2\mathrm{r}}\right)^2}\right), & \text{for } \|x-y\|\le 2\mathrm{r}, \\ 1 & \text{, for } \|x-y\|>2\mathrm{r}. \end{cases}$$

For the Thomas process, it is (see (II.57))

$$g(\|x-y\|)=1+\frac{1}{4\lambda_{P_1}\pi\sigma^2}\exp\left(\frac{-\|x-y\|^2}{4\sigma^2}\right),$$

and for the log-Gaussian process, it is (see (II.43))

$$g(x-y)=\frac{\rho^{(2)}(x,y)}{\rho^2}=\exp\left(\sigma^2\, r(x-y)\right).$$

To generate the log-Gaussian process, we used R, together with the library RandomFields. We used the same method as in [5]: first we approximated the Gaussian field Y by the values of the corresponding finite dimensional Gaussian distribution on a grid 50×50, representing the domain of simulation and then we simulated inhomogeneous Poisson process. For simplicity, we chose for our simulations two simple models as the models for the covariance of the random Gaussian field Y. The first one is the exponential model for which the covariance function is of the form

$$\boldsymbol{cov}(Y(x),Y(y))=\mathit{nugget}+\mathit{variance}\,\exp\left(\frac{-\|x-y\|}{\mathit{scale}}\right),$$

where *nugget*, *variance* and *scale* are the parameters to give. Again, in order to simplify simulations, we chose simple values: we set $\mathit{nugget}=0$, $\mathit{variance}=1$, $\mathit{scale}=0{,}0001$. The choice of the scale is a consequence of (II.43); the scale taking small values, the exponential term is tending to zero and so is

$$\boldsymbol{cov}(Y(x),Y(y))=\exp\left(\frac{-\|x-y\|}{0{,}0001}\right) \text{ and } \boldsymbol{var}(Y)=1.$$

Thus the variability of the intensity ρ of the log-Gaussian process is not too important. As we did band because we used the processes we generated previously we chose $\boldsymbol{E}\,Y = \ln(240)$ to have a total intensity close to 400.Using the same notations as in (II.43), our process is determined by

$$\begin{cases} \_\ \mu = \ln(240) \\ \_\ \sigma^2 = 1 \\ \_\ r(x-y) = \exp(-10000\|x-y\|) \end{cases} \text{ or equivalently } \begin{cases} \_\ \rho = \exp\left(\ln(240) + \frac{1}{2}\right) \\ \_\ g(x-y) = \exp\left(\exp(-10000\|x-y\|)\right) \end{cases}.$$

We chose the wave model as our second model for the covariance of Y and kept the same parameters $nugget = 0$, $variance = 1$, $scale = 0{,}0001$. In this case, it is of the form

$$\boldsymbol{cov}(Y(x), Y(y)) = \frac{\sin\left(\frac{\|x-y\|}{0{,}0001}\right)}{\frac{\|x-y\|}{0{,}0001}} \text{ and } \boldsymbol{var}(Y) = 1,$$

and the process is completely determined by

$$\begin{cases} \_\ \mu = \ln(240) \\ \_\ \sigma^2 = 1 \\ \_\ r(x-y) = \dfrac{\sin(10000\|x-y\|)}{10000\|x-y\|} \end{cases} \text{ or equivalently } \begin{cases} \_\ \rho = \exp\left(\ln(240) + \frac{1}{2}\right) \\ \_\ g(x-y) = \exp\left(\dfrac{\sin(10000\|x-y\|)}{10000\|x-y\|}\right) \end{cases}.$$

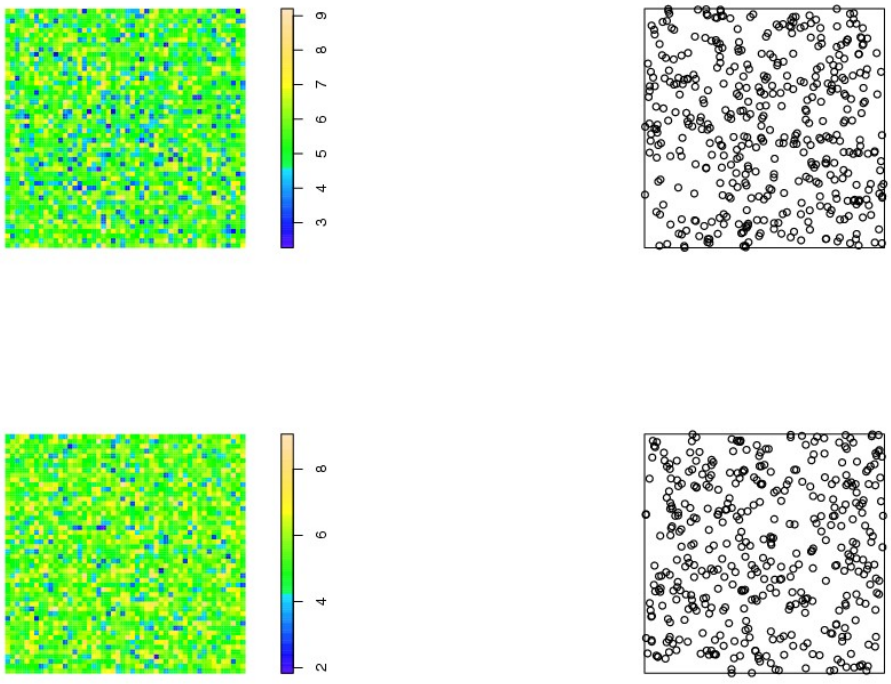

Fig. IV.15: Top: Gaussian random field with mean ln(240) and exponential correlation function (variance 1, scale 0,0001) and the corresponding log-Gaussian Cox process. Bottom: Gaussian random field with mean ln(240) and wave correlation function (variance 1, scale 0,0001) and the corresponding log-Gaussian Cox process.

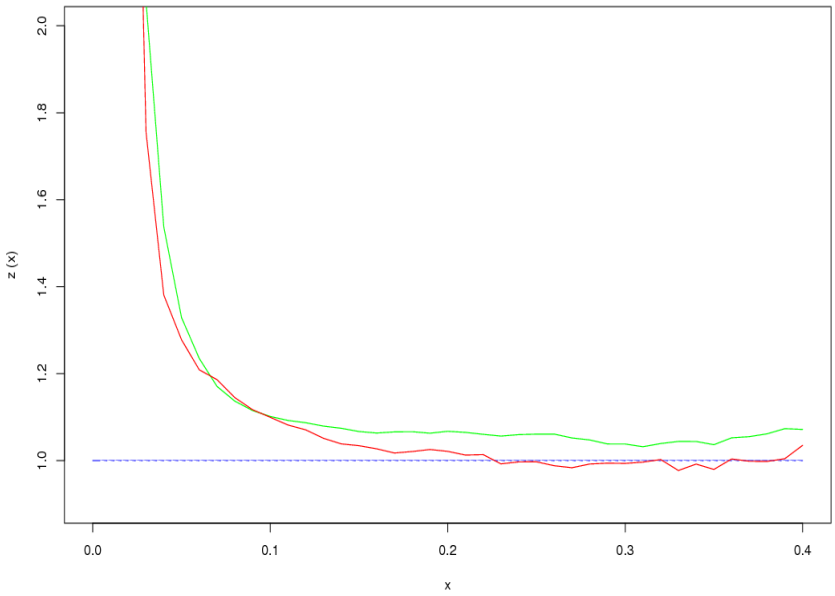

Fig. IV.16: estimate of the z-function for the log-Gaussian Cox process. Green: exponential correlation function for the Gaussian field. Red: wave correlation function.

As we see in *Fig. IV.16* the estimator is not very instructive for small r. It appears to be better in case of a wave correlation function for the Gaussian random field Y than it is in case of an exponential correlation function, but they do not differ much and fit the theoretical model for $r \geq 0{,}15$.

The function was introduced to evaluate the appropriateness of the results obtained in two previous studies [9] and [15], both papers bringing the same conclusion that some observed data set (pine forest) fitted a Matérn cluster model. We thought it would be useful to see how the z-function behaves when considering the Matérn cluster process, and see if there is a clear difference with the results shown in *Fig. IV.16*. We simulated three such processes, with the same intensity of the parent process and the same cluster intensity, the only difference being the length of the cluster radii. The results are shown in *Fig. IV.17*.

The shape of the curves is much different from the one observed before. The function appears to be stable even at small values of r. Nonetheless, it is difficult to make conclusions. Even though the curves are situated further away from the line $y=1$ for values of the radius 0,08 and 0,25 which would tend to confirm that the function could be used to discriminate between the two processes if a doubt is raised, the curve for a radius equal to 0,15 is more problematic. It is not far from the theoretical value of the z-function for the log-Gaussian process (and could certainly be even closer for some value) and when testing observed data, this might lead to a wrong interpretation.

To avoid misinterpretation for similar estimations of the z-functions, the solution may be to look at the process itself and compare it with simulated realizations. We can see from *Fig. IV.15* and *Fig. IV.18* that the realization of the Matérn process with radius 0,15 is significantly different from the realizations of the log-Gaussian processes tested. However, the use of over statistics may be also useful.

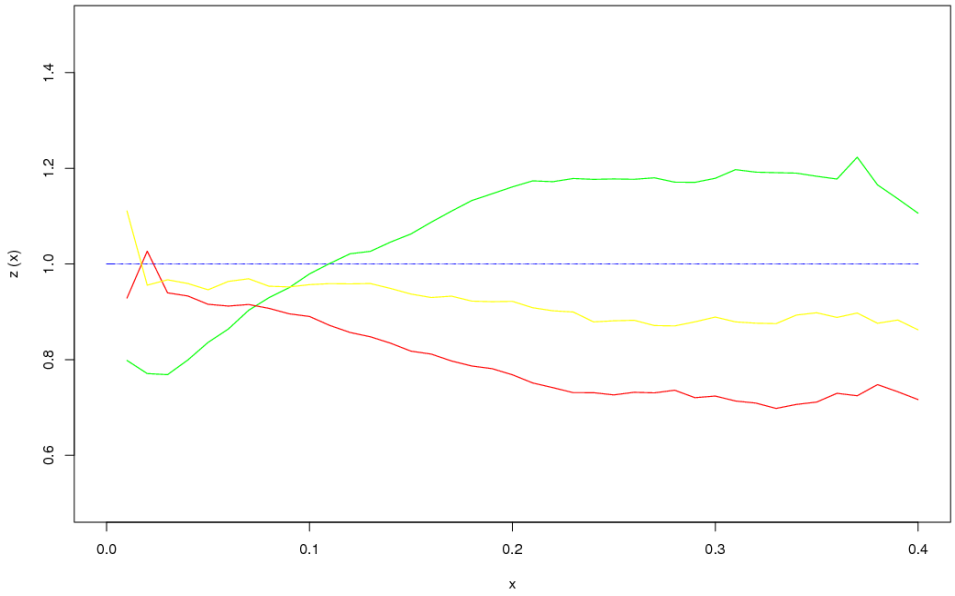

Fig. IV.17: estimators of the z-function for three Matérn cluster point processes with intensity of the parent process equal to 50 and intensity of the clusters 8. Green: radius of the clusters 0,08. Yellow: radius 0,15. Red: radius 0,25.

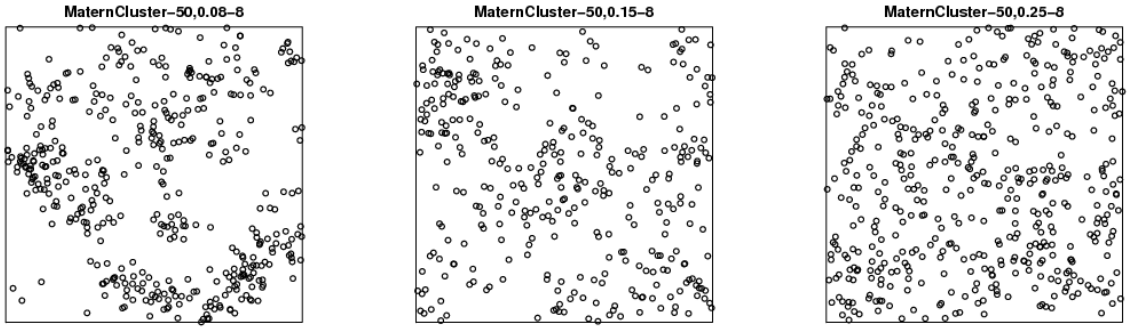

Fig. IV.18: realizations of the three Matérn cluster processes for which the z-function was estimated.

We also tested z for an other cluster process, the Thomas process. We simulated two processes with variance equal to 0,1 and 0,5 respectively. *Fig. IV.19* shows the results obtained for these processes. The process being of the same kind as the Matérn cluster process, the estimators are similar.

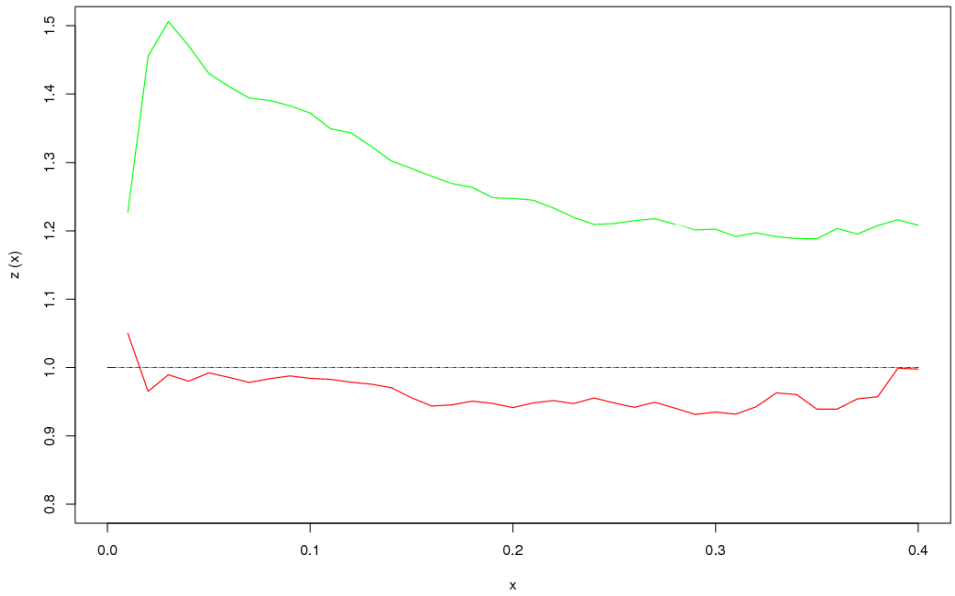

Fig. IV.19: estimated values of z for Thomas processes with intensity of the parent process 50 and cluster intensity 8. Green: variance equal to 0,1. Red: variance equal to 0,5.

To confirm (or, on the contrary, infirm) the doubts we raised on the ability of z to discriminate various processes, we looked at the upper and lower envelopes. We proceeded as follow: we removed from the values we obtained from simulations the smallest and greatest 5% to have a 90% interval of confidence. We drew the upper envelope and the lower envelope (dashed) of the interval but also the arithmetical mean obtained from the values in the interval (dotted). The results are shown in *Fig. IV.20*. The original mean obtained from the use of all calculated values was left to see how important the change was (line).

As shown in the figure, it is clearly difficult to see major differences between processes. May we have data and should we decide which model they best fit, it would be difficult to conclude using this function, the estimate and the envelopes being almost the same, especially for the log-Gaussian and the Thomas processes.

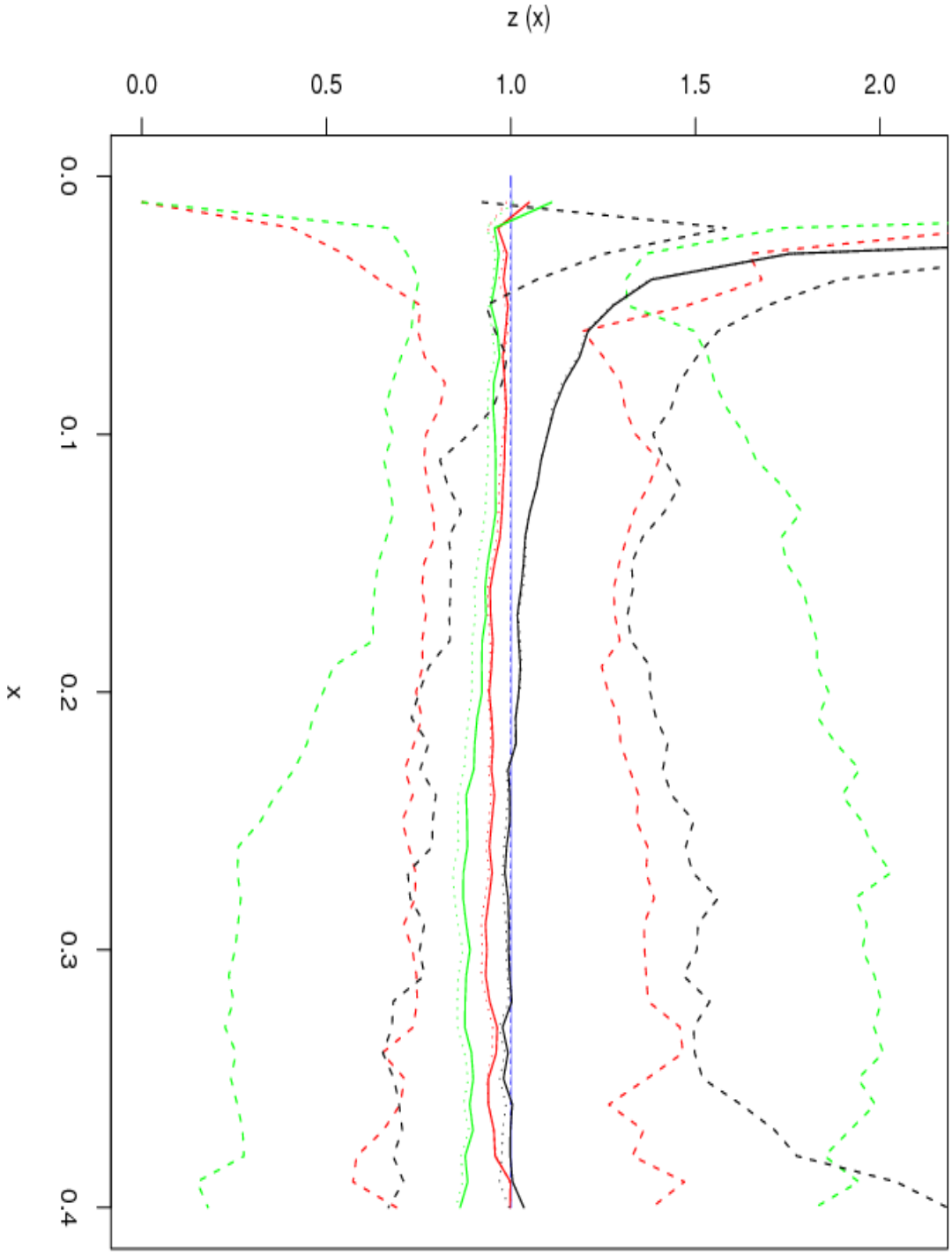

Fig. IV.20: estimates of the z-function and envelopes for log-Gaussian process with wave correlation function for the random field (black), the Matérn cluster process with parameters 50-0,15-8 (green) and the Thomas process with parameters 40-0,5-10 (red).

The article [5] in which the z-function was introduced was published first, the one [12] concerning the T-function coming after. To conclude our study we will look at the results we obtain for the log-Gaussian process when we use T and if this function would not have been better for discriminating the two processes z was thought for.

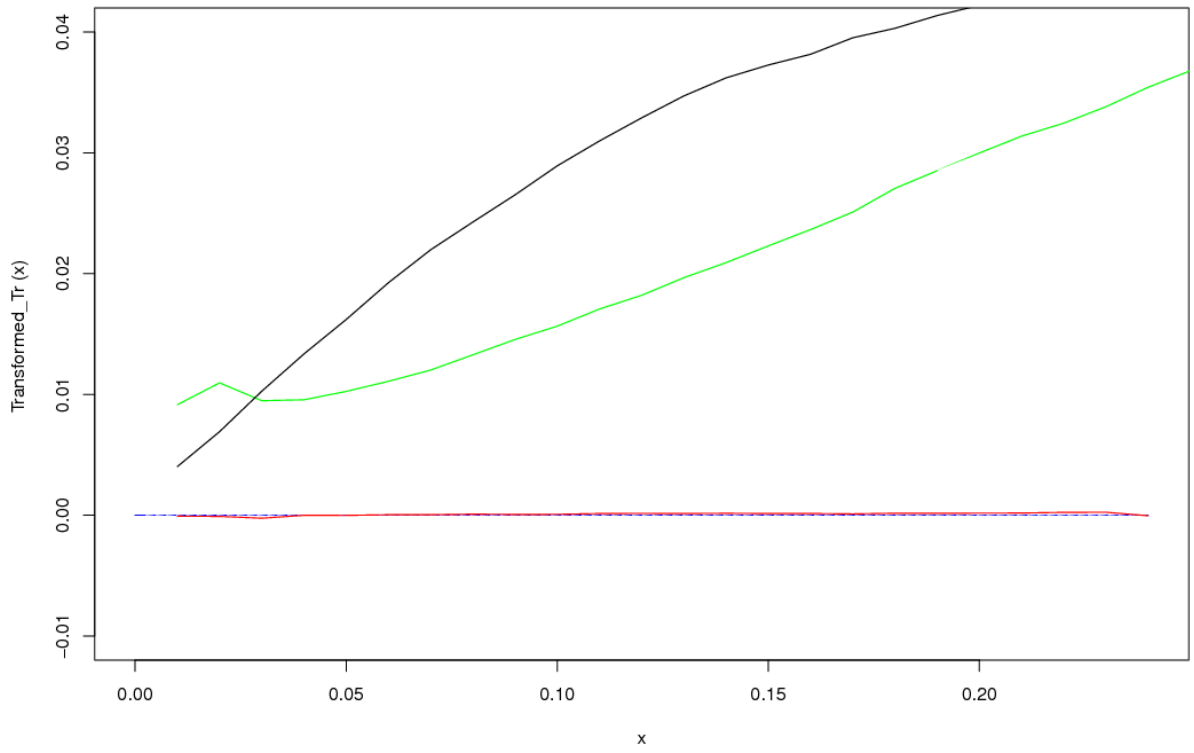

Fig. IV.21: transformed values of the estimator of T. Red: Poisson process with intensity 400. Green: log-Gaussian Cox process ($\mu = \ln(240)$, $r = \exp((10000\sin(\|x-y\|))/(10000\|x-y\|))$). *Black: Matérn cluster process with intensity of the parent process 50, cluster intensity 8 and cluster radii 0,15.*

Whereas we could have had doubts before, results from *Fig. IV.21* clearly show a difference between the two processes. For small values of r, the Matérn process is more clustered than is the log-Gaussian Cox process. On the opposite, the transformed estimate for this last is smaller in the beginning but has apparently a linear growth.

The T-function seems more appropriate for discriminating processes than z, even though it was thought to differentiate a clustered process from a Poisson one and not two clustered processes. It distinguishes well the differences between two different distributions, even distributions of the same kind.

Chapter V

Appendix

Useful recalls (or at least useful for me) of measure theory can be found, for example in [13] (Chapter 1., Mathematical foundation), in [6] (Appendix B, Measure theoretical details) or in [9] (Chapter 2, Lokalne konecne miry na lokalne kompaktnim prostoru and Chapter 3, Nahodne miry: jednoznacnost a existence).

We give here definitions and results on Campbell measures, Palm distributions and Campbell theorems we use in Chapters II and III. These are closely related to moment measures. For our purpose, we will consider the complete separable metric space $(\mathbb{R}^d, \|.\|_d)$ and the point process Ψ on $\mathbb{R}^d$, which maps the probability space (Ω, Σ, P) onto $(N, \mathcal{N})$ and has distribution $Q_\Psi(.)$ and intensity measure $\Lambda_\Psi(.)$.

For any point process Ψ defined as above, we define it's Campbell measure C on $[\mathbb{R}^d \times N, \mathcal{B}^d \times \mathcal{N}]$ by

$$\int \sum_{x \in \psi} f(x, \psi) Q_\Psi(d\psi) = \int \int f(x, \psi) \psi(dx)\, Q_\Psi(d\psi) = \int f(x, \psi)\, C\big(d(x, \psi)\big) \,, \qquad \text{(V.1)}$$

for any strictly positive measurable function f on $[\mathbb{R}^d \times N]$. Similarly, for any function f on $[\mathbb{R}^{nd} \times N]$ satisfying the necessary conditions we spoke about, the n-th order Campbell measure C^n is of the form

$$\int \ldots \int f(x_1, \ldots, x_n, \psi) \psi(dx_1) .. \psi(dx_n)\, Q_\Psi(d\psi) = \int f(x_1, \ldots, x_n, \psi)\, C^n\big(d(x_1, \ldots, x_n, \psi)\big). \qquad \text{(V.2)}$$

Under the same assertions, we can also define the *reduced Campbell measure* $C^!$ of the process

$$\int \sum_{x \in \psi} f(x, \psi \setminus \{x\})\, Q_\Psi(d\psi) = \int f(x, \psi)\, C^!\big(d(x, \psi)\big) \,, \qquad \text{(V.3)}$$

where $\psi \setminus \{x\}$ is a realization of the process Ψ without the point x.

We can also write respectively

$$C(B \times Y) = \int 1_{[\psi \in Y]} \psi(B)\, Q_\Psi(d\psi) = \boldsymbol{E}[\Psi(B), \Psi \in Y], \qquad \text{(V.4)}$$

for any Borel set $B \in \mathcal{B}^d$ and $Y \in \mathcal{N}$ and

$$C^n(B_1\times\ldots\times B_n\times Y)=\boldsymbol{E}[\Psi(B_1),\ldots,\Psi(B_n),\Psi\in Y], \tag{V.5}$$

for any $B_1,\ldots,B_n\in\mathcal{B}^d$ and $Y\in\mathcal{N}$.

From (V.4), we immediately see that whenever Λ_Ψ exists

$$C(.\times\mathcal{N})=\int\psi(.)\,Q_\Psi(d\psi)=\Lambda_\Psi(.), \tag{V.6}$$

so that C determines the first order moment measure Λ_Ψ of the process.

Palm's distributions definition is also derived from the definition of the Campbell measure. Let us suppose that the intensity measure Λ_Ψ of the process is σ-finite, then, following from (V.6), its Campbell measure is also σ-finite. Thus, for each $Y\in\mathcal{N}$ we have

$$C(.\times Y)\le\Lambda_\Psi(.), \tag{V.7}$$

so C is absolutely continuous with respect to the measure Λ_Ψ. By use of the Radon-Nikodym theorem, there exists a Λ-almost surely unique density $P_x\colon x\to P_x(Y)$ such that

$$C(B\times Y)=\int_B P_x(Y)\,\Lambda_\Psi(dx). \tag{V.8}$$

The density is chosen so that

- $P_.(Y)$ is measurable function of x for every $Y\in\mathcal{N}$;
- $P_x(.)$ is a probability measure on $\mathcal{N}$ for every $x\in\mathbb{R}^d$.

P_x is a probability kernel from $(\mathbb{R}^d,\mathcal{B}^d)$ to $(N,\mathcal{N})$. It is called the Palm distribution at x or local Palm distribution for x. Further details for example in [6] (Appendix C, Moment measures and Palm distributions).

For any strictly positive measurable function f on $(\mathbb{R}^d\times N)$, it follows from (V.1) that

$$\int_{\mathcal{N}}\int_X f(x,\psi)\,\psi(dx)\,Q_\Psi(d\psi)=\int_X\int_{\mathcal{N}} f(x,\psi)\,P_x(d\psi)\,\Lambda_\Psi(dx). \tag{V.9}$$

We also define the reduced Campbell measure $C^!$ and the reduced Palm distribution at x $P_x^!$, the last being the density of the first with respect to the intensity measure Λ_Ψ of the process. They are respectively given by

$$\boldsymbol{E}\sum_{x\in\Psi} f(x,\Psi\setminus\{x\})=\int\sum_{x\in\psi} f(x,\psi\setminus\{x\})Q_\Psi(d\psi)=\int f(x,\psi)C^!(d(x,\psi)) \tag{V.10}$$

$$\text{and}\quad C^!(B\times Y)=\int_B P_x^!(Y)\,\Lambda_\Psi(dx), \tag{V.11}$$

for any $B \in \mathcal{B}^d$ and $Y \in \mathcal{N}$.

Using (V.6), we infer the Campbell theorem. For any strictly positive measurable function f on $\mathbb{R}^d$ and any random measure Ψ we have

$$\boldsymbol{E} \sum_{x \in \Psi} f(x) = \int \sum_{x \in \psi} f(x)\, Q_\Psi(d\psi) = \int \int f(x)\psi(dx)\, Q_\Psi(d\psi) = \int f(x)\Lambda_\Psi(dx)\,. \tag{V.12}$$

From (V.6) and Fubini's theorem the definition is correct for f being the indicator function. We proceed in a standard way to prove it for any f defined as above: we use the decomposition $f = f^+ - f^-$ and the fact that a strictly positive measurable function can be expressed in terms of limit.

Using the general definition (V.1) of the Campbell measure and the definition (V.8) of the Palm distribution at x of the process, we introduce the Campbell-Mecke theorem. For any strictly positive measurable function f on $(\mathbb{R}^d \times N)$ and any random measure Ψ we have

$$\begin{aligned} \boldsymbol{E} \sum_{x \in \Psi} f(x, \Psi) &= \int \sum_{x \in \psi} f(x, \psi)\, Q_\Psi(d\psi) \\ &= \int \int f(x, \psi)\, \psi(dx)\, Q_\Psi(d\psi) \\ &= \int \int f(x, \psi)\, C\big(d(x, \psi)\big) \\ &= \int \int f(x, \psi)\, P_x(d\psi)\, \Lambda_\Psi(dx)\,. \end{aligned} \tag{V.13}$$

Again, this theorem is obvious for the indicator function by use of definitions and proceed as above.

For the reduced Campbell measure and reduced Palm distribution that means

$$\begin{aligned} \boldsymbol{E} \sum_{x \in \Psi} f(x, \Psi \setminus \{x\}) &= \int \int f(x, \psi)\, C^!\big(d(x, \psi)\big) \\ &= \int \int f(x, \psi)\, P_x^!(d\psi)\, \Lambda_\Psi(dx)\,. \end{aligned} \tag{V.14}$$

A last important theorem is Slivnyak theorem that gives the Palm distribution P_x at x for a Poisson process Φ. For such a process with distribution P and locally finite intensity measure Λ we have

$$P_x = P * \delta_x\,, \tag{V.15}$$

where $*$ denotes the convolution of measures and δ_x a degenerate random measure at x. That means that the local Palm distribution P_x for a Poisson process Φ coincides with the distribution of the original process with an added non-random point x. Thus, for the reduced Palm distribution it is of the form

$$P_x^! = P\,. \tag{V.16}$$

A proof is available in [13] (example 4.3).

References

[1] Anděl J., *Zakaldy matematicke statistiky*, Ucebni Texty Univerzity Karlovy v Praze

[2] Baddeley A.J., Gill R.D., *Kaplan-Meier Estimators of Distance Distributions for Spatial Point Processes*, The Annales of Statistics Vol. 25, No. 1, 263-292

[3] Baddeley A.J., Silverman B., *A cautionary example on the use of second-order methods for analyzing point patterns*, Biometrics 40, 1089-1094.

[4] Kallenberg O., *Random measures*, Akademie Verlag, Berlin

[5] Moller J., Syversveen A.R., Waagepetersen R.P., *Log Gaussian Cox processes*, Scandinavian Journal of Statistics Vol. 25, 451-482

[6] Moller J., Waagepetersen R.P., *Statistical inference and simulation for spatial point processes*, Monographs on Statistics and Applied Probability 100, Chapman & Hall

[7] Ohser J., *On estimators for the reduced second moment measure of point process*, MOS 14, 63-71

[8] Pawlas Z., *Prostorove modelovani, prostorova statistika*, Ucebni Texty

[9] Penttinen A., Stoyan D., Henttonen H. M., *Marked point processes in forest statistics*, Forest Sci. 38, 806-824

[10] Rataj J., *Bodove procesy*, Ucebni Texty Univerzity Karlovy v Praze

[11] Ripley B.D., *The second-order analysis of stationary point processes*, JAP 13, 255-266

[12] Schladitz K., Baddeley A.J., *A third-order Point process characteristic*, Scandinavian Journal of Statistics Vol. 27, 657-671

[13] Stoyan D., Baddeley A.J. et al., *Case studies in spatial point processes modelling*, Lecture Notes in Statistics 185, Springer

[14] Stoyan D., Kendall W.S., Mecke J., *Stochastic geometry and its applications*, Wiley & Sons

[15] Stoyan D., Stoyan H., *Fractals, random shapes and point fields*, Wiley, Chichester

[16] R Documentation